Table 1 Patient Characteristics and HUT and PET-OEF Parameters

Patient no.	Age (years)	Sex	Transient neurological deficit	Angiographic findings	MRI	HUT					PET OEF (%)
						Minimal/basal MBP (mmHg) (% reduction)	NTG	CMS	Duration to target MBP (min)	Symptoms	
1	64	M	L. amaurosis fugax	L. ICAS	L. occipital	66/120 (45%)	+	–	19	Presyncope	41.1
2	55	M	L. hemiparesis	Bil. MCAO	R. CR	63/116 (46%)	–	–	15	Presyncope	39.4
3	56	F	L. hemiparesis	R. ICAO	R. CR	69/108 (36%)	+	+	33	–	58.4
4	52	M	L. upper limb monoparesis	R. MCAO	None	70/105 (32%)	–	+	26	–	44.1
5	40	F	L. hemiparesis and dysarthria	Bil. MCAO	R. BG	71/104 (32%)	–	+	17	–	50.6
6	62	M	L. hemiparesis and dysarthria	R. MCAS	None	57/116 (51%)	+	–	30	Presyncope	43.2
7	69	F	L. upper/lower limb shaking	R. MCAO	None	73/126 (42%)	+	+	36	L. upper/lower limb shaking	60.7
8	66	M	R. upper limb monoparesis	L. ICAO	L. temporal	70/116 (40%)	+	+	36	–	47.4
9	63	M	R. hemiparesis	L. MCAO	L. CR	72/104 (31%)	–	–	28	R. upper limb weakness	58.1
10	71	M	L. hemiparesis	R. ICAO	None	84/105 (20%)	–	+	18	–	58.0
11	59	F	L. upper/lower limb shaking	R. MCAO	None	56/102 (45%)	+	–	52	Presyncope	47.4
12	28	F	L. hemiparesis	Bil. MCAS	None	68/99 (31%)	–	–	23	–	40.7
13	68	M	L. hemiparesis and dysarthria	Bil. MCAO	Bil. BG-CR	80/107 (25%)	–	–	10	L. upper limb shaking	63.8

HUT, head-up-tilt test; PET, positron emission tomography; OEF, oxygen extraction fraction; MRI shows the lesions of cerebral infarction; MBP, mean blood pressure; NTG, nitroglycerin (0.3 mg) s.l.; CSM, carotid sinus massage; ICAS, internal carotid artery stenosis; Bil, bilakeral; MCAO, middle cerebral artery occlusion; CR, corona radiatal; ICAO, internal carotid artery occlusion; MCAS, middle cerebral artery stenosis; BG, basal ganglia.

HUT test, PET and angiography for determining an operation indication of EC-IC bypass surgery. The study protocol was in accordance with the standard ethics guidelines of Osaka University Graduate School of Medicine.

HUT Test

Stepwise reduction of systemic blood pressure was accomplished by passive postural changes on a head-up tilting table[8,14–17] Patients were allowed to rest quietly in the supine position after instrumentation had been completed. Catheterization of the radial artery of each patient allowed us to monitor continuously the arterial blood pressure. After the patients had rested for a minimum of 10 min, they were then tilted head-up to an angle of 60° for 30 min or until syncope was imminent. The imminence of syncope was recognized by the presyncopal symptoms such as dizziness, nausea, diaphoresis, blurred vision and diplopia. All presyncopal subjects were returned to the supine position before loss of consciousness. When patients showed focal neurological symptoms such as hemiparesis, hemianopia, dysarthria or limb shaking during HUT tests, patients were recognized as positive by HUT test and returned to the supine position. If blood pressure was not sufficiently reduced by this method, patients were given nitroglycerin (0.3 mg, s.l.), and then received carotid sinus massage because this technique can be safely performed even in elderly patients[18] The goal level of mean blood pressure during HUT in the present study was 80 mmHg, above the lower limit of cerebral blood flow (CBF) autoregulation in normal subjects.

PET Imaging

All patients were scanned with a Headtome V/SET 2400W system (Shimadzu Co Ltd), which acquires 63 slices with slice thickness of 3.1 mm, as described previously[19] All scans were performed at a resolution of 3.7 mm full-width at half-maximum in the transaxial direction and at 5 mm in the axial direction. For the ^{15}O-labeled gas steady-state method, $C^{15}O$ (550 MBq/min) and $^{15}O_2$ (1,300 MBq/min) were inhaled through a mask. The scan time was 9 min and arterial blood was manually sampled from the radial artery 4 times during each scan. The concentration of the radiotracer activity in the whole blood and plasma was measured with a well counter; the arterial blood hematocrit, hemoglobin concentration, PaO_2, and $PaCO_2$ were also measured. Inhalation of 2,000 MBq $C^{15}O$ and a 9-min scanning period were used to measure the cerebral blood volume (CBV). Arterial sampling was manually performed 3 times during the scanning, and the radiotracer activity in whole blood was measured. The CBF, cerebral metabolic rate of oxygen ($CMRO_2$), and OEF were calculated from the steady-state method, and $CMRO_2$ and OEF were corrected according to the CBV. All PET data were analyzed with the Dr View pro5.0 image analysis software system (Asahi Kasei Joho System Co Ltd) running on a UNIX system and an Indigo 2 station (Silicon Graphics). Circular regions-of-interest, 20 mm in diameter, were placed over the cortex at the level of the parietal lobe (upper MCA territory) in the PET images of each patient. As the normal values we used PET parameter values obtained from 7 patients without either infarction or severe stenosis/occlusion (<50%) who were suffering from nonspecific brain symptoms without focal signs: CBF, $46.9\pm11.3\ ml\cdot100\ g^{-1}\cdot min^{-1}$ (mean±SD); OEF, 44.1±4.62%; $CMRO_2$, $3.39\pm0.82\ ml\cdot100\ g^{-1}\cdot min^{-1}$; CBV, 4.22±0.75%. The misery perfusion group was identified as OEF >53.3% (mean±2 SD of the mean OEF value). The increased OEF value was compatible with that beyond the upper 95% confidence limits defined in healthy volunteers[6]

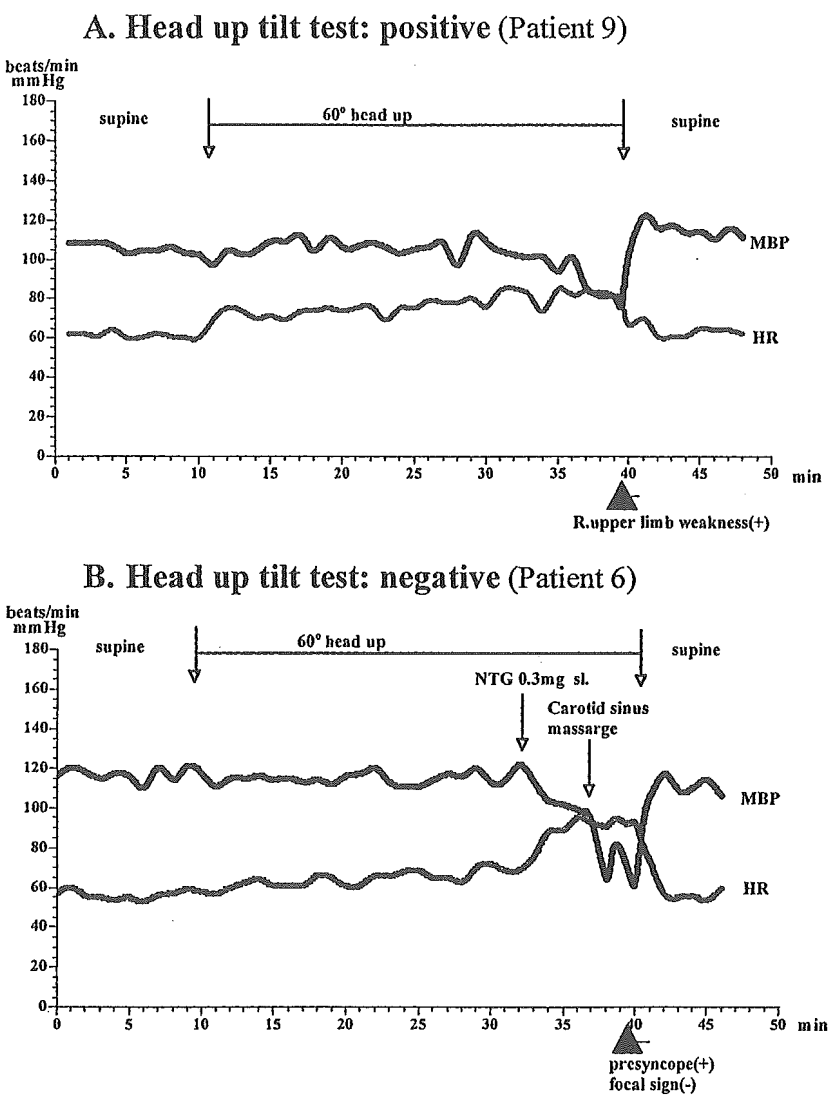

Fig 1. Time course of mean blood pressure (MBP) and heart rate (HR) in head-up-tilt test. (A) Head-up-tilt test: positive (patient 9 in Table 1). A 63-year-old man who complained of weakness of the right lower extremity during walking. MBP started to decline from 104 mmHg during tilting for 28 min. He complained of weakness of the right upper limb when MBP was 72 mmHg. After returning to the supine position, MBP returned to 102 mmHg promptly and his symptoms disappeared within 30 s. (B) Head-up-tilt test: negative (patient 6 in Table 1). After head-up, administration with nitroglycerin (NGT) and carotid sinus massage, MBP declined from 120 mmHg to 65 mmHg at which stage he had presyncopal sensation without focal symptoms.

Results

In 1 of 14 patients, blood pressure did not fall despite orthostatic stress, nitroglycerin administration and carotid sinus massage, and so the patient was excluded from this study.

The clinical characteristics of the 13 patients included in this study are summarized in Table 1. Infarction was found with MRI in 7. In the HUT tests, 3 of the 13 patients showed a transient event such as limb-shaking and hemiparesis (Table 1). Change in blood pressure and heart rate, and clinical symptoms during the HUT test and after return to the sipine position in cases 6 and 9 are shown in Fig 1. Four patients had presyncopal sensation without an event comparable to a previous TIA. Focal symptoms in 3 patients (cases 7, 9 and 13 in Table 1) that appeared during the HUT tests disappeared completely within 60 s after returning to the supine position.

CBF, $CMRO_2$, OEF and CBV values were obtained in the MCA territory of the affected hemisphere of 13 patients (Fig 2). All 3 patients who were HUT positive had OEF >53% (ie, misery perfusion) (Fig 3). In contrast, only 2 of 10 patients without focal symptoms during the HUT test had OEF >53.3%. Therefore, the sensitivity and specificity of the HUT test for predicting patients with misery perfusion were 60% and 100%, respectively. By contrast, no clear cut-off point was found for the CBF, CBV and $CMRO_2$ values between the HUT-positive and -negative groups (Fig 2).

Discussion

In patients with major cerebral arterial occlusive disease, the mechanisms of stroke ipsilateral to the occlusive vessel include embolism from the atherosclerotic plaque and hemodynamic insufficiency[3] Since a large international clinical trial failed to show the efficacy of the EC-IC bypass procedure in preventing stroke,[20] it has been abandoned in most parts of the world. However, this procedure has been shown to be successful, at least, in eliminating repetitive symptoms in patients with hemodynamic TIA?[9-11] Identification of hemodynamic CVD is important for management of carotid occlusion because patients may benefit from therapeutic interventions that improve blood flow to the brain. Because the degree of stenosis or the presence of arterial occlusion does not predict the hemodynamic status

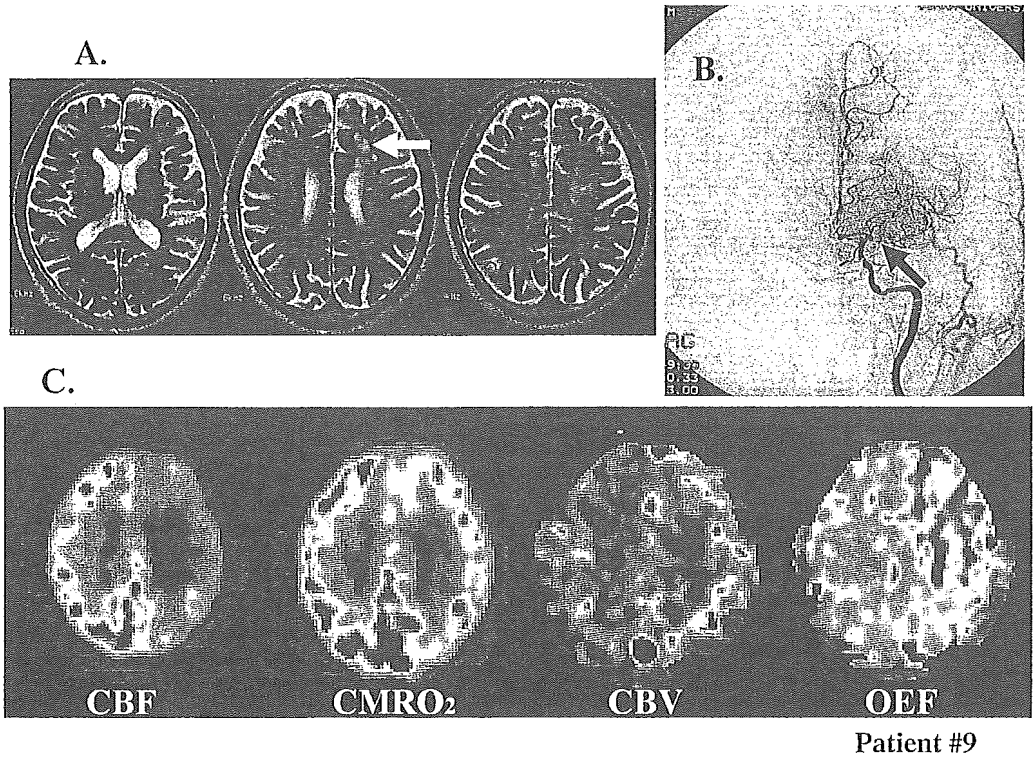

Fig 2. Representative MRI (A), angiography (B) and positron emission tomography (PET) images (C) in a patient with limb weakness during head-up tilt tests and misery perfusion (patient 9 in Table). (A) MRI shows ischemic lesions (white arrow) in the subcortical watershed territory of the left frontal cortex. (B) Carotid angiography shows occlusion of the left middle cerebral artery (arrow). (C) PET images demonstrate decreased cerebral blood flow (CBF), increased cerebral blood volume (CBV) and elevated oxygen extraction fraction (OEF) in the left cerebral hemisphere (OEF=58%).

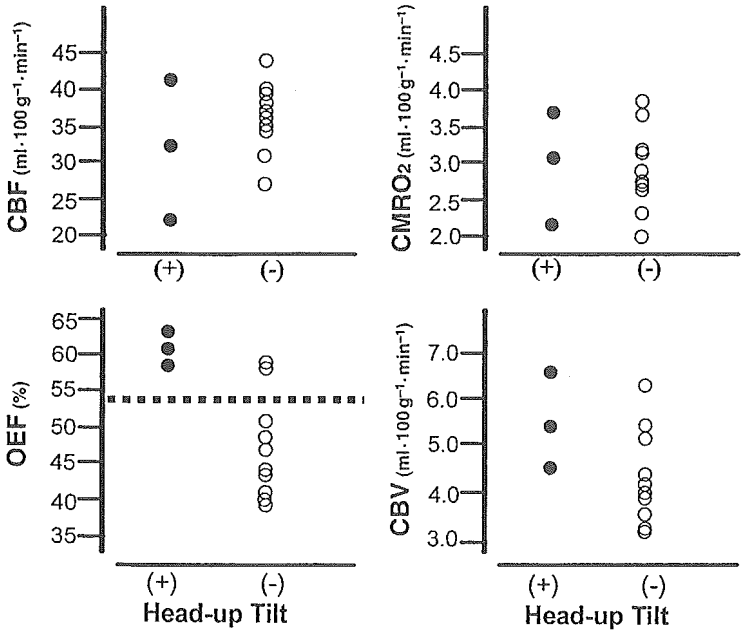

Fig 3. Positron emission tomography (PET) parameters of the territory of the affected middle cerebral artery (MCA) in patients with and without focal symptoms during head-up tilt tests. Closed circles indicate patients who showed focal symptoms during head-up-tilt tests; broken line indicates the OEF cutoff value of 53.3.

of the distal circulation[2] measurement of cerebral hemodynamics by single-photon emission computed tomography[21–23] PET[5,6,24] or transcranial Doppler (TCD)[25] have been used to detect hemodynamic insufficiency. Among several hemodynamic parameters, the OEF obtained in PET is believed to be the most reliable predictor of future stroke in carotid occlusion[1,2] Stage 2, in which CBF is reduced and OEF is increased to maintain $CMRO_2$, has been called "misery perfusion"[4] and represents an inadequate blood supply relative to metabolic demand. It has been dem-

onstrated that the presence of increased OEF is a predictor of subsequent ischemic stroke;[5,6,24] however, the presence of increased OEF does not prove the actual cause of TIA because embolic TIAs can certainly occur in patients with hemodynamic cerebrovascular compromise? Given that hemodynamic CVD affects only a minority of patients with major cerebral artery occlusive lesions, the combination of clinical symptoms and hemodynamic measurement, especially OEF, is presumably the most reliable way of identifying hemodynamic CVD. However, the association between clinical symptoms and OEF has not been carefully examined. Although reduction of CBF and CBF/CBV in the frontal to parietal lobe has been reported[9,11,26] 2 recent studies in patients with ICA occlusion showed no significant differences between patients with and without hemodynamic TIA in any of the hemodynamic parameters on either MRA or in CO_2 reactivity measurement with TCD[27,28]

We used the HUT test to decrease blood pressure safely for the purpose of selecting candidates for EC-IC bypass surgery. Although Tatemichi et al used infusion of trimethaphan to induce hypotension in a patient with bilateral carotid occlusive disease,[11] we prefer orthostatic stress because of the prompt recovery of blood pressure and relief from symptoms by head-down. All 3 patients who were positive in the HUT tests showed misery perfusion on PET (Table 1) and were regarded as having hemodynamic CVD, requiring referral to a neurosurgeon for EC-IC bypass. Increased OEF was observed in 2 of 9 patients without focal signs during the HUT tests and it is unknown whether these patients are at high risk of a hemodynamic incident. The presence of misery perfusion has been shown in longitudinal studies to increase the risk,[5,6] but it is unclear whether the symptoms of these patients are of hemodynamic origin or not.[5,6]

In conclusion, the HUT test was able to detect patients with cerebral hemodynamic insufficiency and the combination of the HUT test and cerebral hemodynamic measurement could be useful as an operation indication for EC-IC bypass.

References

1. Klijn CJM, Kappelle LJ, Tulleken CAF, van Gijn J. Symptomatic carotid artery occlusion: A reappraisal of hemodynamic factors. *Stroke* 1997; **28:** 2084–2093.
2. Derdeyn CP, Grubb RL, Powers WJ. Cerebral hemodynamic inpairment: Methods of measurement and association with stroke risk. *Neurology* 1999; **53:** 251–259.
3. Hankey GJ, Warlow CP. Prognosis of symptomatic carotid artery occlusion: An overview. *Cerebrovasc Dis* 1991; **1:** 245–256.
4. Baron JC, Bousser MG, Rey A, Guillard A, Comar D, Castaigne P. Reversal of focal "misery-perfusion syndrome" by extra-intracranial arterial bypass in hemodynamic cerebral ischemia: A case study with ^{15}O positron emission tomography. *Stroke* 1981; **12:** 454–459.
5. Grubb RL, Derdeyn CP, Fritsch SM, Carpenter DA, Yundt KD, Videen TO, et al. Importance of hemodynamic factors in the prognosis of symptomatic carotid occlusion. *JAMA* 1998; **280:** 1055–1060.
6. Yamauchi H, Fukuyama H, Nagahama Y, Nabatame H, Ueno M, Nishizawa S, et al. Significance of increased oxygen extraction fraction in five-year prognosis of major cerebral arterial occlusive diseases. *J Nucl Med* 1999; **40:** 1992–1998.
7. Powers WJ. Cerebral hemodynamics in ischemic cerebrovascular disease. *Ann Neurol* 1991; **29:** 231–240.
8. Carey BJ, Manktelow BN, Panerai RB, Potter JF. Cerebral autoregulation responses to head-up tilt in normal subjects and patients with recurrent vasovagal syncope. *Circulation* 2001; **104:** 898–902.
9. Yanagihara T, Piepgras DG, Klass DW. Repetitive involuntary movement associated with episodic cerebral ischemia. *Ann Neurol* 1985; **18:** 244–250.
10. Baquis GD, Pessin MS, Scott RM. Limb shaking: A carotid TIA. *Stroke 1985*; **16:** 444–448.
11. Tatemichi TK, Young WL, Prohovnik I, Gitelman DR, Correll JW, Mohr JP. Perfusion insufficiency in limb-shaking transient ischemic attacks. *Stroke* 1990; **21:** 341–347.
12. Whisnant JP, Basford JR, Bernstein EF. Classification of cerebrovascular disease III. *Stroke* 1990; **21:** 637–676.
13. Shimizu Y, Kitagawa K, Nagai Y, Narita M, Hougaku H, Masuyama T, et al. Carotid atherosclerosis as a risk factor for complex aortic lesions in patients with ischemic cerebrovascular disease. *Circ J* 2003; **67:** 597–600.
14. Matsushita K, Kuriyama Y, Nagatsuka K, Nakamura M, Sawada T, Omae T. Periventricular white matter lucency and cerebral blood flow autoregulation in hypertensive patients. *Hypertension* 1994; **23:** 565–568.
15. Novak V, Novak P, Spies JM, Low PA. Autoregulation of cerebral blood flow in orthostatic hypotension. *Stroke* 1998; **29:** 104–111.
16. Dan DD, Hoag JB, Ellenbogen KA, Wood MA, Eckberg DL, Gilligan DM. Cerebral blood flow velocity declines before arterial pressure in patients with orthostatic vasovagal presyncope. *J Am Coll Cardiol* 2002; **39:** 1039–1045.
17. Suwa S, Sumiyoshi M, Mineda Y, Ohta H, Kojima S, Nakata Y. Vasovagal response induced by a low dose of isoproterenol infusion before tilting-up. *Circ J* 2004; **68:** 876–877.
18. Richardson DA, Bexton R, Shaw FE, Steen N, Bond J, Kenny RA. Complications of carotid sinus massage: A prospective series of older patients. *Age Ageing* 2000; **29:** 413–417.
19. Imaizumi M, Kitagawa K, Hashikawa K, Oku N, Teratani T, Takasawa M, et al. Detection of misery perfusion with split-dose ^{123}I-iodoamphetamine single-photon emission computed tomography in patients with carotid occlusive diseases. *Stroke* 2002; **33:** 2217–2223.
20. The EC-IC Bypass Study Group. Failure of extracranial–intracranial arterial bypass to reduce the risk of ischemic stroke: Results of an international randomized trial. *N Engl J Med* 1985; **313:** 1191–1200.
21. Yokota C, Hasegawa Y, Minematsu K, Yamaguchi T. Effect of acetazolamide reactivity and long-term outcome in patients with major cerebral artery occlusive diseases. *Stroke* 1998; **29:** 640–644.
22. Kuroda S, Houkin K, Kamiyama H, Mitsunori K, Iwasaki Y, Abe H. Long-term prognosis of medically treated patients with internal carotid or middle cerebral artery occlusion: Can acetazolamide test predict it? *Stroke* 2001; **32:** 2110–2116.
23. Ogasawara K, Ogawa A, Terasaki K, Shimizu H, Tominaga T, Yoshimoto T. Use of cerebrovascular reactivity in patients with symptomatic major cerebral artery occlusion to predict 5-year outcome: Comparison of xenon-133 and iodine-123-IMP single-photon emission computed tomography. *J Cereb Blood Flow Metab* 2002; **22:** 1142–1148.
24. Derdeyn CP, Videen TO, Yundt KD, Fritsch SM, Carpenter DA, Grubb RL, et al. Variability of cerebral blood volume and oxygen extraction: Stages of cerebral hemodynamic impairment revisited. *Brain* 2002; **125:** 595–607.
25. Markus H, Cullinane M. Severely impaired cerebrovascular reactivity predicts stroke and TIA risk in patients with carotid artery stenosis and occlusion. *Brain* 2001; **124:** 457–467.
26. Gibbs JM, Wise RJS, Leeders KL, Jones T. Evaluation of cerebral perfusion reserve in patients with carotid-artery occlusion. *Lancet* 1984; **1:** 310–314.
27. van Everdingen KJ, Visser GH, Klijin CJM, Kappelle LJ, van der Grond J. Role of collateral flow on cerebral hemodynamics in patients with unilateral internal carotid artery occlusion. *Ann Neurol* 1998; **44:** 167–176.
28. Klijn CJM, Kappelle LJ, van der Grond J, Visser GH, Algra A, Tulleken CAF, et al. Lack of evidence for a poor haemodynamic or metabolic state of the brain in patients with haemodynamic clinical features associated with carotid artery occlusion. *Cerebrovasc Dis* 2001; **12:** 99–107.

Relations of Serum High-Sensitivity C-Reactive Protein and Interleukin-6 Levels With Silent Brain Infarction

Taku Hoshi, MD; Kazuo Kitagawa, MD, PhD; Hiroshi Yamagami, MD, PhD; Shigetaka Furukado, MD; Hidetaka Hougaku, MD, PhD; Masatsugu Hori, MD, PhD

Background and Purpose—Small silent brain infarction (SBI) is often found on magnetic resonance (MR) images of apparently healthy individuals at cardiovascular risk. Particularly, small SBI found in subcortical white matter, basal ganglia, or thalamus is thought to be caused by cerebral small vessel disease. Although several lines of evidence suggest a role of inflammatory processes in atherothrombotic vascular events, their involvement in SBI remains to be determined. This study examines the associations between serum inflammatory markers and SBI as a manifestation of cerebral small vessel disease.

Methods—One hundred ninety-four patients without histories of cardiovascular accidents were prospectively enrolled for this study. All patients underwent brain MR imaging and carotid ultrasonography, and patients with SBI diagnosed underwent further MR angiography. As common inflammatory markers, serum levels of high-sensitivity C-reactive protein (hsCRP) and interleukin-6 (IL-6) were evaluated.

Results—SBIs were found in 40 patients, and all of those were located in subcortical and infratentorial area, without MR angiographic evidence for obstructive lesions in proximal cerebral arteries. Mean hsCRP and IL-6 levels were higher in patients with SBI than in those without. Also, higher levels of both hsCRP (odds ratio [OR], 1.85 per standard deviation [SD] increase) and IL-6 (OR, 2.00/SD increase) were associated with higher likelihood for SBI. Moreover, the associations were only slightly attenuated when adjusting traditional cardiovascular risk factors and carotid IMT.

Conclusions—Higher levels of hsCRP and IL-6 appear to be associated with small SBI, suggesting a role of inflammatory processes in cerebral small vessel disease. (***Stroke.* 2005;36:768-772.**)

Key Words: inflammation ■ interleukins ■ magnetic resonance imaging

Silent brain infarction (SBI), often seen on brain magnetic resonance (MR) images of healthy elderly individuals, is associated with increased risk for stroke and cognitive decline.[1] In previous studies, >90% of such SBIs were small (<15 mm in diameter) and found in subcortical white matter, basal ganglia, thalamus, or infratentorial region.[2–5] Also, autopsy studies have shown that cerebral small vessel disease underlies such asymptomatic brain lesions.[6–8] Although several risk factors have been identified for the occurrence of SBI, including age, hypertension, diabetes,[5,9,10] homocysteine,[11–13] and carotid intima-media thickness,[14,15] whether inflammatory processes are involved in its cause remains to be determined

Recent studies in vascular biology have shown that chronic inflammation plays a crucial role in the development of atherosclerosis.[16] Particularly, several lines of evidence suggest the value of measuring serum levels of inflammatory markers, such as high-sensitivity C-reactive protein (hsCRP) and interleukin-6 (IL-6), for predicting stroke and other cardiovascular events.[17–20] Additionally, such inflammatory markers have been associated with plaque progression and its instability in large arteries.[21,22] However, we are unaware of studies investigating the involvement of inflammation in SBI.

In the current study, we examine the associations of hsCRP and IL-6 with SBI in neurologically asymptomatic patients at cardiovascular risk to explore the relationships between inflammation and cerebral small vessel disease.

Patients and Methods

Patients

The subjects for this study were enrolled from neurologically asymptomatic patients who consecutively visited the Department of Internal Medicine and Therapeutics at Osaka University Hospital between April 2002 and December 2003. The majority of patients had been referred from another hospital or department for the risk assessment and primary prevention of stroke. At the time of referral, comprehensive neurological evaluations were performed by our stroke neurologists, including physical and psychological examinations. When no neurological signs/symptoms were identified, patients were found to be candidates for this study. Thus, patients with histories of stroke or other neurological disease were not included in

Received August 12, 2004; final revision received December 13, 2004; accepted January 11, 2005.

From the Division of Stroke Medicine, Department of Internal Medicine and Therapeutics (A8), Osaka University Graduate School of Medicine, Osaka, Japan.

Correspondence to Taku Hoshi, MD, Division of Stroke Medicine, Department of Internal Medicine and Therapeutics (A8), Osaka University Graduate School of Medicine. 2-2 Ymada-oka, Suita, Osaka 565-0871, Japan. E-mail thoshi@medone.med.osaka-u.ac.jp

Stroke **is available at http://www.strokeaha.org** **DOI: 10.1161/01.STR.0000158915.28329.51**

the study sample. Additionally, patients who had ever experienced nonspecific neurological symptoms, such as dizziness, vertigo, headache, tinnitus, and syncope, were included, but only if the symptoms were not present at the time of neurological evaluations. Given the nature of study sample, many of the patients had cardiovascular risk factors, including hypertension, hyperlipidemia, and diabetes.

During the study period, 236 patients were found to be potential candidates for this study. However, patients with ischemic heart disease (n=24) or peripheral vascular disease (n=7) were excluded. Additionally, patients with collagen disease (n=5), malignant disease (n=2), or acute viral infection (n=4) were excluded, because such conditions could increase the levels of inflammatory markers, potentially modifying the relationships between inflammatory markers and SBI. Consequently, this study comprised 194 neurologically asymptomatic patients (mean±standard deviation age, 67.3±7.5 years) who subsequently underwent brain MR imaging.

This study was approved by the Ethics Committee of Osaka University Graduate School of Medicine. All patients gave written informed consent before entry to the current study.

Diagnosis of SBI

All MR imaging was performed with 1.5-T Signa Horizon (GE Medical Systems) or 1.5-T Magnetom Vision (Siemens). The whole brain was scanned, and 20 axial images were produced; slice thickness was 5 mm and interslice gap was 2 mm. The imaging protocol was consisted of a T2-weighted spin-echo (repetition time/echo time [TR/TE]=5000/130 ms), T1-weighted spin-echo (TR/TE=500/9 ms), and fluid-attenuated inversion-recovery (TR/TE=8000/155 ms, inversion time=2000 ms) imaging.

A single trained physician who was blinded to patients' clinical details evaluated the existence, location, and size of brain infarcts on MR images. Thereby, SBI was defined as an area of focal hyperintensity on T2-weighted images with corresponding low signal intensity on T1-weighted images, which was ≥3 mm in diameter. Also, the diagnosis was made only when such a lesion was surrounded by hyperintense gliotic rim on fluid-attenuated inversion-recovery images to exclude dilated perivascular space.

When patients had SBI diagnosed, they subsequently underwent MR angiography to explore the existence of large vessel disease that could explain the cause of SBI.

Measurement of Serum Inflammatory Markers

After MR examination, blood was drawn with minimally traumatic venipuncture for measurement of serum inflammatory markers. Blood was then centrifuged at 3000 rpm at 4°C for 15 minutes, and aliquots were stored at −70°C. Circulating hsCRP was measured by latex turbidimetric immunoassay with a sensitivity of 0.01 mg/dL (Shionogi Biomedical Laboratory Inc). Serum IL-6 was measured by enzyme-linked immunosorbent assay (High Sensitivity Quantikine kit; R&D System). The detectable limit for IL-6 was 0.10 pg/mL.

Evaluation of Cardiovascular Risk Factors

Supine blood pressure was measured before the MR imaging examination. Fasting blood glucose, serum total cholesterol, high-density lipoprotein cholesterol, triglycerides, and serum creatinine levels were determined from the blood sample taken for inflammatory marker evaluation. Information on patient medical history and medication use was obtained from the clinical records, with investigators blinded to the MR findings. Hypertension was defined by casual blood pressure ≥140/90 mm Hg or by current use of antihypertensive agents. Diabetes mellitus was defined by fasting blood glucose level ≥7.0 mmol/L or by use of glucose-lowering agents. Hyperlipidemia was defined by fasting serum total cholesterol level >5.7 mmol/L, triglycerides level >1.7 mmol/L, or by use of cholesterol-lowering agents. Smoking status was evaluated based on self-reports. Patients were categorized according to their smoking habits as nonsmoker (never smoked) or ever-smoker (smoked habitually at some time in their lives).

Evaluation of Carotid Atherosclerosis

Duplex carotid ultrasonography was performed to evaluate the severity of carotid atherosclerosis. All ultrasound examinations were performed with a Phillips SONOS 5500 equipped with a 7.5-MHz linear-array transducer. The intima-media thickness (IMT), defined as the distance between the intimal-luminal interface and the medial-adventitial interface, was measured as previously described.[23] We calculated the mean carotid artery IMT (mean IMT) by averaging the thickness at 12 sites: the near and far walls of both the right and left distal common carotid artery, carotid bifurcation, and internal carotid artery.

Statistical Analyses

Because the distributions of hsCRP and IL-6 levels appeared to be left-skewed, they were normalized by logarithmic transformation. To analyze the associations between inflammatory markers and patient characteristics, we used Pearson correlation analysis and 2-sample t test. To compare prevalence of SBI by the tertile of hsCRP and IL-6, we used χ^2 test. To analyze the relation between SBI and patient characteristics, we used χ^2 test for categorical data and 2-sample t test for continuous data. Odds ratio was calculated for the likelihood of SBI by multivariate logistic regression analyses, in which logarithmically transformed values of inflammatory markers were used. Of note, odds ratio was shown per standard deviation in log (inflammatory marker) increase. Probability values were 2-tailed, and values of $P<0.05$ were considered significant. All statistical analyses were performed with SPSS 11.5J (SPSS Japan Inc).

Results

Patient Characteristics

Forty patients (21%) were found to have 1 or more SBIs on MR images (26 patients had a single infarct, whereas 14 had from 2 to 8 infarcts). Also, 50% of infarcts were located in the subcortical white matter (corona radiata, centrum semiovale, subcortical frontal, temporal and parietal lobes), and 45% were in the basal ganglia and thalamus (Figure 1). No patients had cortical infarcts in the study sample. Additionally, all infarcts (n=72) were <15 mm in diameter, and 97% of those were <10 mm. By MR angiographic examinations, 38 of 40 patients had no significant obstructive lesions in the proximal cerebral arteries. Although 2 patients had stenotic lesions (50% to 75%) in the horizontal portion of middle cerebral arteries, they were on the contralateral side to SBI.

Relation Between SBI and Inflammatory Markers

By univariate analysis, age, BMI, prevalence of hypertension, and systolic blood pressure were higher in patients with SBI than in those without, and so were hsCRP and IL-6 levels (Table 1). Additionally, prevalence of SBI was higher in the highest tertile of hsCRP level than in the lowest or middle tertile (Figure 2). Also, the prevalence was higher in the middle and highest tertiles of IL-6 level than in the lowest tertile.

Associations between inflammatory markers levels and SBI are summarized in Table 2. In unadjusted analysis, each 1 SD greater log hsCRP and each 1 SD greater log IL-6 were associated with 1.85-fold and 2.00-fold higher likelihood for SBI, respectively. Adjustments for age and sex modified these associations only slightly (model 1). After additional adjustments for traditional cardiovascular risk factor and medication use (model 2), both hsCRP and IL-6 remained to be associated with SBI. After further adjustments for mean IMT (model 3), these associations persisted.

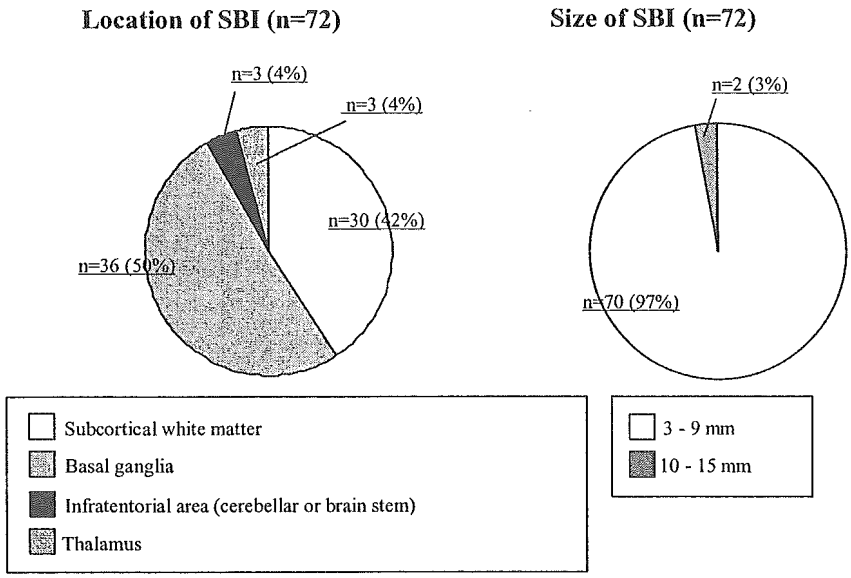

Figure 1. Distribution of infarct location and size in patients with silent brain infarct on MR imaging.

Discussion

Recently, SBI has attracted much attention because it increases the risk for future stroke[1] and dementia.[2,4] In the present study, levels of hsCRP and IL-6 were higher in patients with SBI than in those without. Also, higher levels of such markers were associated with higher likelihood for SBI. To the best of our knowledge, this is the first study that demonstrates the associations between inflammatory markers and SBI.

TABLE 1. Baseline Characteristics of Patients With and Without Silent Brain Infarction

		Silent Brain Infarction		
Index	All Patients (n=194)	No (n=154)	Yes (n=40)	*P* Value
Age, y	67.3±7.5	66.5±7.6	70.6±6.0	0.002
Male sex, no. (%)	93 (48)	69 (45)	24 (60)	0.087
BMI, kg/m2	23.0±2.7	22.8±2.6	23.8±3.3	0.03
Hypertension, no. (%)	128 (66)	94 (61)	34 (85)	0.004
Diabetes mellitus, no. (%)	31 (16)	21 (14)	10 (25)	0.081
Hyperlipidemia, no. (%)	130 (67)	101 (66)	29 (73)	0.4
Atrial fibrillation, no. (%)	5 (3)	3 (2)	2 (5)	0.6
Ever smoker, no. (%)	78 (40)	59 (38)	19 (48)	0.3
Systolic blood pressure, mm Hg	137.3±15.0	135.3±14.6	145.1±14.4	<0.001
Diastolic blood pressure, mm Hg	81.4±10.0	81.3±10.0	81.8±9.9	0.7
Total cholesterol, mmol/L	5.50±0.83	5.54±0.85	5.41±0.75	0.3
HDL cholesterol, mmol/L	1.54±0.41	1.50±0.39	1.46±0.41	0.5
Triglyceride, mmol/L	1.45±0.67	1.44±0.68	1.31±0.56	0.3
Fasting blood glucose, mmol/L	5.63±1.02	5.58±1.02	5.79±1.03	0.3
Serum creatinine, mg/dL	0.80±0.40	0.76±0.24	0.95±0.73	0.1
Mean IMT, mm	0.99±0.24	0.97±0.23	1.05±0.26	0.054
Medication use, no. (%)	105 (54)	81 (53)	24 (60)	0.4
Inflammatory marker				
High-sensitivity CRP, mg/dL	0.13±0.42 (0.05)	0.08±1.69 (0.04)	0.33±0.86 (0.08)	0.004
Interleukin-6, pg/mL	2.08±3.57 (1.32)	1.67±1.96 (1.20)	3.63±6.69 (1.89)	<0.001
Mini-Mental State Examination	28.1±2.0	28.1±2.2	28.0±1.6	0.6

Values are unadjusted mean±SD (median) or no. of patients (percentage).

P values are χ^2 test for the categorical data, and 2 sample *t* test for the continuous data.

Medication use means the percentage of patients who are using at least one anti-inflammation agent; Aspirin, HMG-CoA reductase inhibitors, angiotensin converting enzyme-inhibitors and angiotensin receptor blockers.

*Statistical tests performed in logarithmically transformed variables.

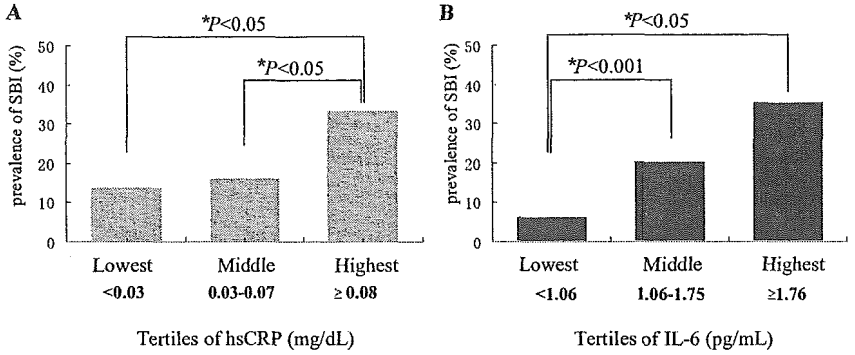

Figure 2. Prevalence (%) of silent brain infarction (SBI) by tertile of high-sensitivity CRP (lowest, <0.03 mg/dL; middle, 0.03 to 0.07 mg/dL; highest, ≥0.08 mg/dL) (A), and interleukin-6 (lowest, <1.06 pg/mL; middle, 1.06 to 1.75 pg/mL; highest, ≥1.76 pg/mL) (B). *P computed by χ^2 analysis.

In previous studies, prevalence of SBI is reported to be 10.6% to 24.8% in apparently healthy individuals.[1,2,9,10,12] In the current study, 21% (40 out of 194) patients were found to have SBI, which is not surprising when the nature of our study sample is taken into account. Also, 95% of SBIs were located in the subcortical white matter, basal ganglia, or thalamus, and 97% of those were <10 mm (Figure 1). These findings are consistent with the commonly known features of SBI. Moreover, MR angiographic examinations revealed no significant obstructive lesions that could explain the occurrence of such SBI. Taken together, SBI found in this study is likely to be the manifestation of cerebral small vessel disease.

Previous studies have shown associations of SBI with age, hypertension, and diabetes.[5,9,10] In line with such studies, age and prevalence of hypertension were higher in patients with SBI than in those without (Table 1). Also, hsCRP and IL-6 levels were higher in SBI patients than in those without (Table 1), suggesting an enhanced level of chronic inflammation in SBI patients. Moreover, prevalence of SBI increased in a stepwise fashion across the tertiles of hsCRP and IL-6 levels (Figure 2). Additionally, increases in such inflammatory markers were associated with higher likelihood for SBI (Table 2, model 1), and the associations persisted when traditional cardiovascular risk factors were adjusted (Table 2, model 2). These findings suggest the link between inflammation and SBI. Of note, recent studies have shown associations of SBI with carotid atherosclerosis.[14,15] Given such studies, we have performed additional analysis with carotid IMT taken into account. When such parameters were included in the model (Table 2, model 3), the association between inflammatory markers and SBI were only slightly modified, further supporting their linkages.

Our findings suggest that inflammation is related to pathologic changes in cerebral small vessels that cause lacunar infarction. By measuring soluble plasma markers (eg, soluble intercellular adhesion molecule-1, soluble endothelial leukocyte adhesion molecule, and thrombomodulin), previous studies have shown inflammatory endothelial activation and endothelial dysfunction in patients with cerebral small vessel disease.[25,26] Also, autopsy examinations revealed migration of foamy macrophages in the vessel walls of cerebral arterioles together with hyaline thickening and ectasia of parenchymal arteries in 15 out of 20 patients with ischemic vascular dementia.[27] These clinical and autopsy studies may support our result. In other words, although whether inflammatory endothelial activation induces arteriolosclerosis and lipohyalinosis is not established, it is likely that chronic inflammatory response in cerebral small vessels is involved in the pathology of this microangiopathy.

This study has some limitations. First, because the current study is cross-sectionally designed, we cannot refer to the causal relationships between inflammatory markers and SBI. Second, recent studies have reported that elevated level of plasma homocysteine is associated with the risk factor for SBI,[11–13,28] which could potentially impact on the relationships between inflammatory markers and SBI. Third, although SBI found in this study is likely to represent cerebral small vessel disease, possibility of cardiogenic or arteriogenic emboli cannot be completely denied. Taken together, extensive prospective studies are necessary to establish the link between inflammation and cerebral small vessel disease.

In conclusion, this study demonstrates that levels of circulating hsCRP and IL-6 are associated with SBI independent of traditional cardiovascular risk factors, suggesting an involvement of inflammation in cerebral small vessel disease.

TABLE 2. OR (95% CI) for The Prevalence of SBI According to Levels of Inflammatory Markers

	Multivariate Logistic Regression Analysis			
	Unadjusted OR (95% CI)	Model 1 OR (95% CI)	Model 2 OR (95% CI)	Model 3 OR (95% CI)
hsCRP, mg/dL per SD in log (hsCRP) increase	1.85 (1.29–2.63)	1.73 (1.20–2.51)	1.49 (1.00–2.22)	1.50 (1.00–2.24)
IL-6, pg/mL per SD in log (IL-6) increase	2.00 (1.39–2.88)	1.87 (1.29–2.71)	1.85 (1.24–2.78)	1.85 (1.24–2.78)

Model 1, adjusted for age and sex.
Model 2, adjusted for age, sex, BMI, smoking, hypertension, diabetes mellitus, hyperlipidemia and medication use.
Model 3, adjusted for age, sex, BMI, smoking, hypertension, diabetes mellitus, hyperlipidemia, medication use and mean IMT.
SD for log (hsCRP)=0.55; SD for log (IL-6)=0.30.

Acknowledgments

The present study was supported in part by the Smoking Research Foundation of Japan. We thank A. Kanzawa, M. Ikusawa, S. Imoto, and R. Morimoto for their secretarial assistance.

References

1. Vermeer SE, Hollander M, van Dijk EJ, Hofman A, Koudstaal PJ, Breteler MM. Silent brain infarcts and white matter lesions increase stroke risk in the general population: the Rotterdam scan study. *Stroke.* 2003;34:1126–1129.
2. Giele JL, Witkamp TD, Mali WP, van der Graaf Y. Silent brain infarcts in patients with manifest vascular disease. *Stroke.* 2004;35:742–746.
3. Kario K, Matsuo T, Kobayashi H, Hoshide S, Shimada K. Hyperinsulinemia and hemostatic abnormalities are associated with silent lacunar cerebral infarcts in elderly hypertensive subjects. *J Am Coll Cardiol.* 2001;37:871–877.
4. Hougaku H, Matsumoto M, Kitagawa K, Harada K, Oku N, Itoh T, Maeda H, Handa N, Kamada T. Silent cerebral infarction as a form of hypertensive target organ damage in the brain. *Hypertension.* 1992;20: 816–820.
5. Vermeer SE, Den Heijer T, Koudstaal PJ, Oudkerk M, Hofman A, Breteler MM. Incidence and risk factors of silent brain infarcts in the population-based Rotterdam scan study. *Stroke.* 2003;34:392–396.
6. Fisher CM. The arterial lesions underlying lacunes. *Acta Neuropathol (Berl).* 1968;12:1–15.
7. Tuszynski MH, Petito CK, Levy DE. Risk factors and clinical manifestations of pathologically verified lacunar infarctions. *Stroke.* 1989;20: 990–999.
8. Shinkawa A, Ueda K, Kiyohara Y, Kato I, Sueishi K, Tsuneyoshi M, Fujishima M. Silent cerebral infarction in a community-based autopsy series in Japan. The hisayama study. *Stroke.* 1995;26:380–385.
9. Kobayashi S, Okada K, Koide H, Bokura H, Yamaguchi S. Subcortical silent brain infarction as a risk factor for clinical stroke. *Stroke.* 1997;28: 1932–1939.
10. Longstreth WT, Jr., Bernick C, Manolio TA, Bryan N, Jungreis CA, Price TR. Lacunar infarcts defined by magnetic resonance imaging of 3660 elderly people: the cardiovascular health study. *Arch Neurol.* 1998;55: 1217–1225.
11. Kim NK, Choi BO, Jung WS, Choi YJ, Choi KG. Hyperhomocystinemia as an independent risk factor for silent brain infarction. *Neurology.* 2003;61:1595–1599.
12. Matsui T, Arai H, Yuzuriha T, Yao H, Miura M, Hashimoto S, Higuchi S, Matsushita S, Morikawa M, Kato A, Sasaki H. Elevated plasma homocysteine levels and risk of silent brain infarction in elderly people. *Stroke.* 2001;32:1116–1119.
13. Vermeer SE, van Dijk EJ, Koudstaal PJ, Oudkerk M, Hofman A, Clarke R, Breteler MM. Homocysteine, silent brain infarcts, and white matter lesions: the Rotterdam scan study. *Ann Neurol.* 2002;51:285–289.
14. Shinoda-Tagawa T, Yamasaki Y, Yoshida S, Kajimoto Y, Tsujino T, Hakui N, Matsumoto M, Hori M. A phosphodiesterase inhibitor, cilostazol, prevents the onset of silent brain infarction in japanese subjects with type II diabetes. *Diabetologia.* 2002;45:188–194.
15. Kawamura T, Umemura T, Kanai A, Uno T, Matsumae H, Sano T, Sakamoto N, Sakakibara T, Nakamura J, Hotta N. The incidence and characteristics of silent cerebral infarction in elderly diabetic patients: association with serum-soluble adhesion molecules. *Diabetologia.* 1998; 41:911–917.
16. Ross R. Atherosclerosis—an inflammatory disease. *N Engl J Med.* 1999; 340:115–126.
17. Volpato S, Guralnik JM, Ferrucci L, Balfour J, Chaves P, Fried LP, Harris TB. Cardiovascular disease, interleukin-6, and risk of mortality in older women: the women's health and aging study. *Circulation.* 2001;103: 947–953.
18. Ridker PM, Cushman M, Stampfer MJ, Tracy RP, Hennekens CH. Inflammation, aspirin, and the risk of cardiovascular disease in apparently healthy men. *N Engl J Med.* 1997;336:973–979.
19. Cesari M, Penninx BW, Newman AB, Kritchevsky SB, Nicklas BJ, Sutton-Tyrrell K, Rubin SM, Ding J, Simonsick EM, Harris TB, Pahor M. Inflammatory markers and onset of cardiovascular events: results from the health ABC study. *Circulation.* 2003;108:2317–2322.
20. Ridker PM, Rifai N, Stampfer MJ, Hennekens CH. Plasma concentration of interleukin-6 and the risk of future myocardial infarction among apparently healthy men. *Circulation.* 2000;101:1767–1772.
21. Hashimoto H, Kitagawa K, Hougaku H, Shimizu Y, Sakaguchi M, Nagai Y, Iyama S, Yamanishi H, Matsumoto M, Hori M. C-reactive protein is an independent predictor of the rate of increase in early carotid atherosclerosis. *Circulation.* 2001;104:63–67.
22. Yamagami H, Kitagawa K, Nagai Y, Hougaku H, Sakaguchi M, Kuwabara K, Kondo K, Masuyama T, Matsumoto M, Hori M. Higher levels of interleukin-6 are associated with lower echogenicity of carotid artery plaques. *Stroke.* 2004;35:677–681.
23. Sakaguchi M, Kitagawa K, Nagai Y, Yamagami H, Kondo K, Matsushita K, Oku N, Hougaku H, Ohtsuki T, Masuyama T, Matsumoto M, Hori M. Equivalence of plaque score and intima-media thickness of carotid ultrasonography for predicting severe coronary artery lesion. *Ultrasound Med Biol.* 2003;29:367–371.
24. Vermeer SE, Prins ND, den Heijer T, Hofman A, Koudstaal PJ, Breteler MM. Silent brain infarcts and the risk of dementia and cognitive decline. *N Engl J Med.* 2003;348:1215–1222.
25. Fassbender K, Bertsch T, Mielke O, Muhlhauser F, Hennerici M. Adhesion molecules in cerebrovascular diseases. Evidence for an inflammatory endothelial activation in cerebral large- and small-vessel disease. *Stroke.* 1999;30:1647–1650.
26. Hassan A, Hunt BJ, O'Sullivan M, Parmar K, Bamford JM, Briley D, Brown MM, Thomas DJ, Markus HS. Markers of endothelial dysfunction in lacunar infarction and ischaemic leukoaraiosis. *Brain.* 2003;126: 424–432.
27. Vinters HV, Ellis WG, Zarow C, Zaias BW, Jagust WJ, Mack WJ, Chui HC. Neuropathologic substrates of ischemic vascular dementia. *J Neuropathol Exp Neurol.* 2000;59:931–945.
28. Hassan A, Hunt BJ, O'Sullivan M, Bell R, D'Souza R, Jeffery S, Bamford JM, Markus HS. Homocysteine is a risk factor for cerebral small vessel disease, acting via endothelial dysfunction. *Brain.* 2004;127: 212–219.

Adenovirus-Mediated Gene Transfer of Heparin-Binding Epidermal Growth Factor-Like Growth Factor Enhances Neurogenesis and Angiogenesis After Focal Cerebral Ischemia in Rats

Shiro Sugiura, MD; Kazuo Kitagawa, MD, PhD; Shigeru Tanaka, MD, PhD; Kenichi Todo, MD; Emi Omura-Matsuoka, MD; Tsutomu Sasaki, MD, PhD; Takuma Mabuchi, MD, PhD; Kohji Matsushita, MD, PhD; Yoshiki Yagita, MD, PhD; Masatsugu Hori, MD, PhD

Background and Purpose—Recent studies have demonstrated that neurotrophic factors promote neurogenesis after cerebral ischemia. However, it remains unknown whether administration of genes encoding those factors could promote neural regeneration in the striatum and functional recovery. Here, we examined the efficacy of intraventricular injection of a recombinant adenovirus-expressing heparin-binding epidermal growth factor-like growth factor (HB-EGF) on neurogenesis, angiogenesis, and functional outcome after focal cerebral ischemia.

Methods—Transient focal ischemia was induced by middle cerebral artery occlusion (MCAO) for 80 minutes with a nylon filament in Wistar rats. Three days after MCAO, either adenovirus-expressing HB-EGF (Ad-HB-EGF) or Ad-LacZ, the control vector, was injected into the lateral ventricle on the ischemic side. Bromodeoxyuridine (BrdU) was injected intraperitoneally twice daily on the sixth and seventh days. On the eighth or 28th day after MCAO, we evaluated infarct volume, neurogenesis, and angiogenesis histologically. Neurological outcome was serially evaluated by the rotarod test after MCAO.

Results—There was no significant difference in infarct volume between the 2 groups. Treatment with Ad-HB-EGF significantly increased the number of BrdU-positive cells in the subventricular zone on the 8th day. In addition, on the 28th day, BrdU-positive cells differentiated into mature neurons in the striatum on the ischemic side but seldom the cells given Ad-LacZ. Enhancement of angiogenesis at the peri-infarct striatum was also observed on the eighth day in Ad-HB-EGF–treated rats. Treatment with Ad-HB-EGF significantly enhanced functional recovery after MCAO.

Conclusions—Our data suggest that gene therapy using Ad-HB-EGF contributes to functional recovery after ischemic stroke by promoting neurogenesis and angiogenesis. (***Stroke*. 2005;36:859-864.)**

Key Words: angiogenesis ■ cerebral ischemia ■ growth factors ■ gene therapy ■ neurogenesis

Because neurotrophic and growth factors such as epidermal growth factor (EGF),[1] fibroblast growth factor-2 (FGF-2),[2] and brain-derived neurotrophic factor (BDNF)[3] have been shown to be implicated in neurogenesis as well as neuroprotection in vivo, recent studies have focused on promoting endogenous neurogenesis by these factors as a novel therapeutic strategy against ischemic stroke.[4,5] However, because most of these therapeutic peptides do not pass through the blood–brain barrier and their half lives are relatively short, continuous or repeated intracerebral or intraventricular infusion would be necessary. Meanwhile, intracerebral gene transfer can result in efficient local production of therapeutic molecules for a longer period by a single injection, overcoming such disadvantages of infection caused by retention of catheters and brain damage caused by repeated injections. Furthermore, Matsuoka et al reported recently that adenovirus-mediated intraventricular gene transfer of FGF-2, which increased FGF-2 level in brain tissues and the cerebrospinal fluid (CSF), is more effective in promoting neurogenesis after ischemia than continuous infusion of FGF-2 peptide, which increased FGF-2 level only in the CSF.[6]

Heparin-binding epidermal growth factor-like growth factor (HB-EGF), a member of the EGF family, was originally identified as a macrophage-derived mitogenic and chemotactic factor, which is initially synthesized as a membrane-anchored form, proHB-EGF, and released as a secreted form, soluble HB-EGF.[7] In the central nervous system, HB-EGF is widely distributed in neurons and neuroglia throughout the brain.[8] However, the expression of HB-EGF in the subventricular zone (SVZ) gradually decreases and finally disap-

Received October 8, 2004; final revision received December 2, 2004; accepted January 11, 2005.

From the Division of Strokology, Department of Internal Medicine and Therapeutics, Osaka University Graduate School of Medicine, Suita, Japan.

Correspondence to Shiro Sugiura, MD, Division of Strokology, Department of Internal Medicine and Therapeutics (A8), Osaka University Graduate School of Medicine, 2-2, Yamadaoka, Suita City, Osaka, 565-0871, Japan. E-mail siro@medone.med.osaka-u.ac.jp

Stroke **is available at http://www.strokeaha.org** **DOI: 10.1161/01.STR.0000158905.22871.95**

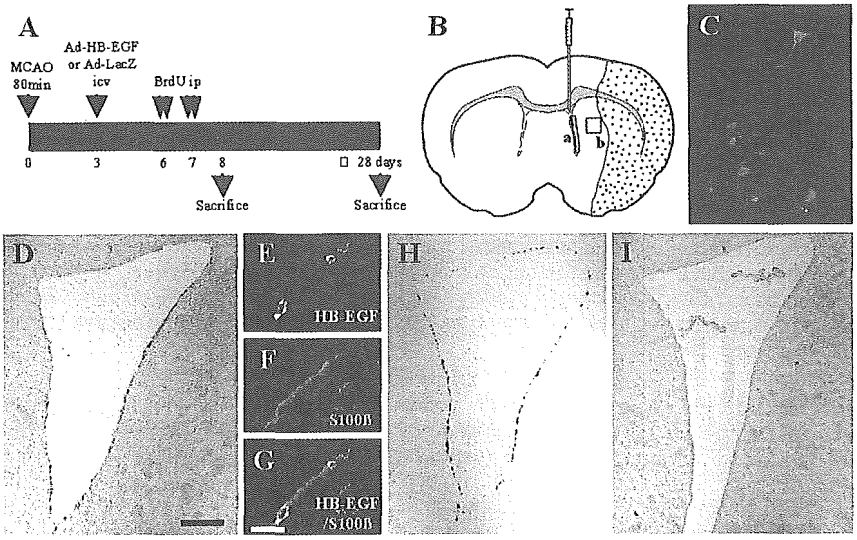

Figure 1. A, Experimental protocol. B, Diagram of the brain sections. Adenoviral vector was injected into the lateral ventricle. Infarct area is shown as stippled area. For quantification of neurogenesis and angiogenesis, ROIs were defined in the SVZ (a) and striatum (b). C, Adenoviral gene expression of HB-EGF was confirmed in HEK 293 cells. D, In vivo expression of exogenous HB-EGF could be observed at the periventricular area in Ad-HB-EGF–treated rats. E to G, Expression of exogenous HB-EGF (red in E and G) was observed mainly in S100β-positive ependymal cells (green in F and G). H and I, In Ad-LacZ–treated rats, Xgal-positive (H) but no HB-EGF–positive cells (I) were detected in the similar pattern. Bar=200 μm in D, H, and I. Bar=20 μm in E through G.

pears as development proceeds.[9] HB-EGF is also induced by cerebral ischemia[10] and stimulates neurogenesis in vitro and in vivo.[11] Recent studies have demonstrated that intraventricular injections of HB-EGF could modify neurogenesis in the SVZ after focal ischemia.[12] However, it is unknown whether HB-EGF can improve neurological function when administered after the expansion of infarct lesion is completed, or whether proliferating neuronal precursors can differentiate into mature neurons.

Furthermore, angiogenesis also plays an important role in the process of tissue remodeling after ischemic stroke. Although the implication of HB-EGF in angiogenesis has been reported in vitro and in vivo,[13] there are few reports about the effects of HB-EGF in angiogenesis after ischemic stroke.

The aim of the present study was to investigate the effects of adenovirus-mediated HB-EGF gene transfer on neurogenesis and angiogenesis in the striatum after focal ischemia.

Materials and Methods

Adenoviral Vector Production

Full-length mouse HB-EGF cDNA, provided by Dr S. Takashima (Osaka University Graduate School of Medicine, Japan), was cloned into an adenoviral vector (Ad-HB-EGF) using Adeno-X expression system (BD Biosciences CLONTECH). Ad-LacZ was used as a control vector. These viral vectors were propagated in human embryonic kidney 293 (HEK 293) cells. Viral titer was determined by use of the Adeno-X rapid titer kit (BD Biosciences CLONTECH) on HEK 293 cells.

To confirm adenovirus-mediated expression of HB-EGF in vitro, HEK 293 cells were treated with Ad-HB-EGF or Ad-LacZ (1.1×10^7 plaque forming units [pfu]/mL) for 48 hours. After fixation with 3% paraformaldehyde, cells were incubated with goat polyclonal anti–HB-EGF antibody (1:200; Santa Cruz Biotechnology, Santa Cruz, Calif) at 4°C overnight and fluorescein isothiocyanate (FITC)–conjugated donkey anti-goat IgG antibody (1:400; Chemicon, Temecula, Calif) at room temperature for 40 minutes.

Animals and Surgical Procedures

Adult male Wistar Rats (Charles River; Yokohama, Japan) weighing 250 to 300 g were used in this study. The experimental protocol was approved by the institutional animal care and use committee of Osaka University Graduate School of Medicine.

Transient Focal Ischemia

Left middle cerebral artery occlusion (MCAO) was produced by the intraluminal filament technique.[14] Eighty minutes after MCAO, rats were reanesthetized with halothane and the occluding filament was withdrawn. Rectal temperature was maintained at 37±0.5°C using a heat lamp during ischemia.

Adenoviral Vector Delivery

Three days after transient MCAO (Figure 1A), rats were anesthetized with 1% halothane and placed in a stereotaxic frame (Summit Medical). A small hole was drilled through the skull, and Ad-HB-EGF or Ad-LacZ (1.1×10^{10} pfu/mL) was injected into the left lateral ventricle (0.4 mm anterior to the bregma, 1.0 mm lateral to the midline, 4.0 mm beneath the dura) in a volume of 10 μL over 10 minutes using a Hamilton microsyringe (Figure 1B). The needle was left in place for an additional 5 minutes and removed slowly over 5 minutes. To evaluate temporal change of the expression of exogenous genes preliminarily, several rats were euthanized at 1, 2, 3, 5, 7, 14, and 25 days after injection of the vectors (n=2 or 3 each).

BrdU Labeling

To label the proliferating cells in the SVZ and striatum, rats were given bromodeoxyuridine (BrdU; 50 mg/kg IP; Sigma) twice daily on the sixth and seventh day after MCAO (Figure 1A).

Motor Function Test

Using the rotarod test, rats were given training sessions on an accelerating rod from 5 to 15 rpm for 3 days before MCAO, and only the rats that were able to stay on the rotating rod at 15 rpm for 200 seconds were subjected to MCAO. Test sessions consisted of 4 trials at 15 rpm and were performed just before MCAO and at 2 hours, 2, 8, 14, 21, and 28 days after MCAO by an investigator who was blinded to the experimental groups. If the rats managed to maintain their balance for 200 seconds, the trial was ended. The final score was expressed as the mean time that a rat was able to remain on the rod for the 4 trials.

Histological Evaluation

At 8 (n=8 per each group) or 28 days (n=8 per each group) after MCAO, the rats were perfused transcardially with Zamboni's solution (2% paraformaldehyde and 0.2% picric acid) under deep pentobarbital anesthesia, and the brains were processed into frozen 10-μm-thick coronal sections as described previously.[14]

Infarct Volume

Infarct volume was evaluated using hematoxylin and eosin–stained specimens from 5 coronal sections per rat, as described previously.[15]

Specimens were obtained 1 mm apart, starting with a section 3 mm rostral to the bregma.

Exogenous Gene Expression

To confirm the exogenous gene expression, X-gal staining for β-galactosidase was performed as described previously.[16] Immunohistochemical staining was performed by using goat polyclonal anti–HB-EGF antibody (1:100), biotinylated rabbit anti-goat IgG antibody (1:200; Vector Laboratories, Burlingame, Calif), and an avidin-biotinylated enzyme complex system (ABC Elite Kit; Vector Laboratories) to detect the expression of HB-EGF. The peroxidase color reaction was developed with 3-amino-9-ethylcarbazole (AEC) solution (Vector Laboratories). To identify the cells expressing exogenous HB-EGF, double immunostaining with mouse monoclonal anti-S-100β antibody (1:200; Sigma, St Louis, Mo), a marker for ependymal cells in the periventricular area and astrocytes,[17] was performed.

Neurogenesis and Angiogenesis

BrdU immunohistochemistry was performed as described previously.[14] Reaction products were visualized with AEC solution. To assess neuronal phenotype of BrdU-positive cells, double immunostaining was performed with the following primary antibodies: rat monoclonal anti-BrdU (1:100; Harlan Sera-lab, Leicestershire, UK), mouse monoclonal anti-rat Nestin (1:100; BD PharMingen, San Jose, Calif), goat polyclonal anti-doublecortin (DCX; 1:100; Santa Cruz Biotechnology), mouse monoclonal anti–β-tubulin III (Tuj-1; 1:200; Research Diagnostics, Flanders, NJ), mouse monoclonal anti–microtubule-associated protein 2 (MAP2; 1:100; Sigma), and mouse monoclonal anti-neuronal nuclei (NeuN; 1:100; Chemicon) antibody. After incubation with primary antibodies at 4°C overnight, sections were incubated with FITC- and rhodamine-conjugated secondary antibodies (1:200; Chemicon) for 1 hour at room temperature. Double immunofluorescence was evaluated using laser confocal-scanning microscopy (LSM 510; Zeiss). To confirm the expression of the receptor of HB-EGF, double immunostaining with rabbit polyclonal anti–EGF-receptor/avian erythroblastic leukemia viral oncogene homolog 1 (EGF-R/ErbB1; 1:100; Santa Cruz Biotechnology) and anti-BrdU, anti-Nestin or anti-DCX antibodies was performed. For evaluation of angiogenesis, double immunostaining with anti-BrdU (1:100) and rabbit polyclonal anti-laminin (1:100; Sigma) antibodies was performed similarly as above.

Quantification

Regions of interest (ROIs) were defined as a zone with 250 μm width and 2000 μm length in the SVZ for counting $BrdU^+$, $Nestin^+BrdU^+$, and DCX^+BrdU^+ cells, and as a box with 700 μm width and length in the peri-infarct striatum for counting $NeuN^+BrdU^+$ and $laminin^+BrdU^+$ cells, as shown in Figure 1B. Four sections, including the caudoputamen, were obtained every 150 μm beginning at a section 1500 μm rostral to the bregma, and the results were expressed as the average number per rat. For measurement of vascular density, each laminin-immunostained coronal section was digitized using a ×20 objective via the NIH Image 1.61 program. Vascular density was calculated by dividing the area of laminin-positive vessels by the total area of the ROIs in the striatum.

Statistical Analysis

All values are expressed as mean±SD. Statistical analysis was performed using SPSS system, version 9.0J. Cell numbers were analyzed by Student *t* test. Rotarod data were analyzed by repeated-measures ANOVA and Mann–Whitney *U* test. $P<0.05$ was considered statistically significant.

Results

Adenovirus-Mediated Gene Expression In Vitro and In Vivo

Expression of HB-EGF by HEK 293 cells treated with Ad-HB-EGF was detected (Figure 1C), whereas no HB-EGF–positive cell was observed in Ad-LacZ–treated HEK 293 cells (data not shown). In vivo expression of exogenous HB-EGF could be detected at the periventricular area, beginning at 1 day, peaking at 3 days, and decreasing slowly toward 14 days after Ad-HB-EGF injection was given (Figure 1D). A month after injection, HB-EGF–positive cells were no longer detected at the periventricular area. Although the number was much smaller, HB-EGF–positive cells were also detected in the contralateral periventricular area 3 days after Ad-HB-EGF injection. Double immunostaining revealed that transgene was expressed mainly in ependymal cells (Figure 1E through 1G). In Ad-LacZ–treated rats, Xgal-positive but

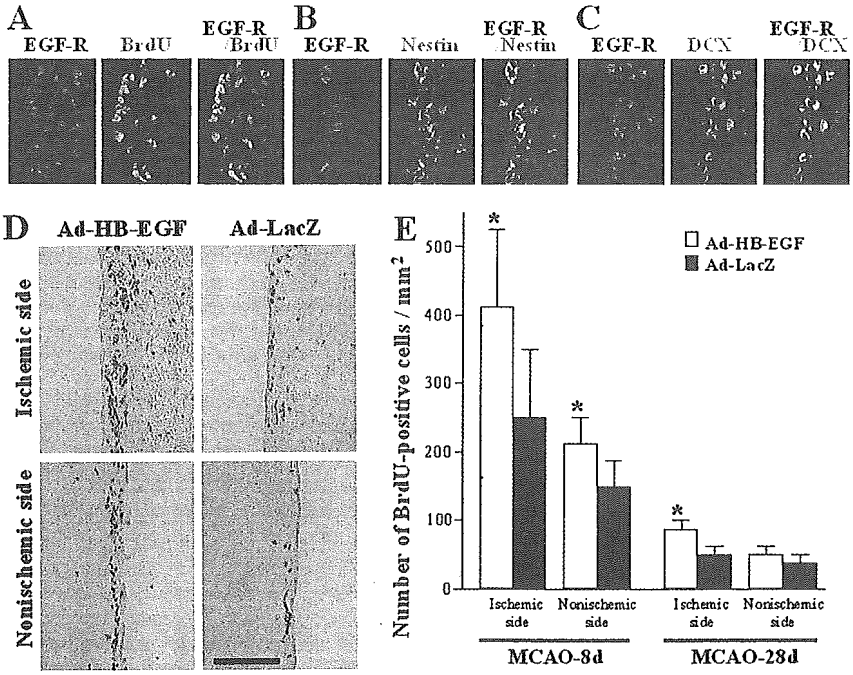

Figure 2. Most of BrdU-positive (A), Nestin-positive (B), and DCX-positive cells (C) in the SVZ expressed EGF-R at 8 days after MCAO. Representative photographs show BrdU-positive cells in the SVZ at 8 days after MCAO (D). In Ad-HB-EGF treatment group, the number of BrdU-positive cells in the SVZ increased not only 8 days but also 28 days after MCAO, especially on the side of the injection (E). *$P<0.05$ vs Ad-LacZ–treated rats at each condition. Bar=100 μm.

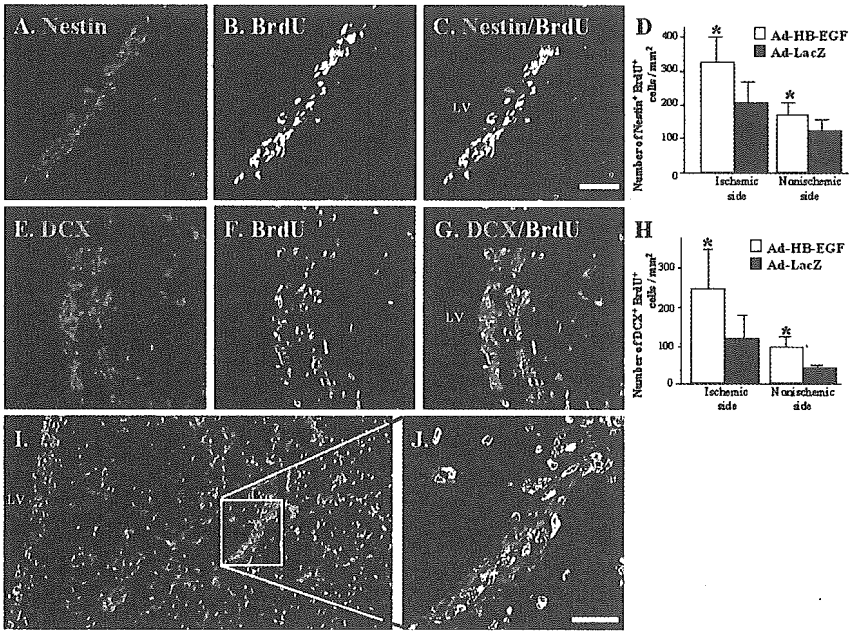

Figure 3. Proliferation and migration of neuronal stem/progenitor cells. Ad-HB-EGF administration increased the number of Nestin$^+$BrdU$^+$ (A through C) and DCX$^+$BrdU$^+$ cells (E through G) in the SVZ at 8 days. Quantitative data of each cell are shown in D and H. Chain migration of DCX$^+$BrdU$^+$ cells into the ischemic boundary of the striatum was enhanced by administration of Ad-HB-EGF at 8 days after MCAO (I and J, corresponding to the box in I). *$P<0.05$ vs Ad-LacZ–treated rats at each condition. Bar=50 μm in A, B, C, E, F, and G. Bar=25 μm in J. LV indicates lateral ventricle.

no HB-EGF–positive cells were detected in a similar pattern (Figure 1H and 1I).

Infarct Volume

There was no significant difference in infarct volume between Ad-HB-EGF– and Ad-LacZ–treated rats at 8 and 28 days after MCAO (52.5±12.9% versus 50.1±13.9%, $P=0.74$ at 8 days; 38.4±12.7 versus 41.8±18.8%, $P=0.72$ at 28 days).

Cell Proliferation in the SVZ and Migration in the Striatum

The expression of EGF-R was observed in most of BrdU-positive, Nestin-positive and DCX-positive cells in the SVZ at 8 days (Figure 2A through 2C). In the Ad-HB-EGF–treated group, the number of BrdU-positive cells in the ipsilateral SVZ increased not only 8 days (406±110 versus 236±92 cells/mm^2; $P<0.05$) but also 28 days after MCAO (79±20 versus 41±24 cells/mm^2; $P<0.05$) compared with Ad-LacZ–treated group (Figure 2D and 2E). Ad-HB-EGF administration also increased the number of BrdU-positive cells that were Nestin positive (322±81 versus 207±64 cells/mm^2; $P<0.05$; Figure 3A through 3D) and DCX-positive (246±101 versus 118±58 cells/mm^2; $P<0.05$; Figure 3E through 3H) on the eighth day. An increase in the number of Nestin$^+$BrdU$^+$ and DCX$^+$BrdU$^+$ cells was observed even in the contralateral SVZ. Moreover, after Ad-HB-EGF administration, there was more enhanced chain migration of DCX$^+$BrdU$^+$ cells into the ischemic boundary of the striatum (Figure 3I and 3J) than was observed in the Ad-LacZ group.

Differentiation of Proliferating Cells and Angiogenesis in the Striatum

Double immunostaining showed that part of BrdU-positive cells in the striatum of the ischemic side colocalized with

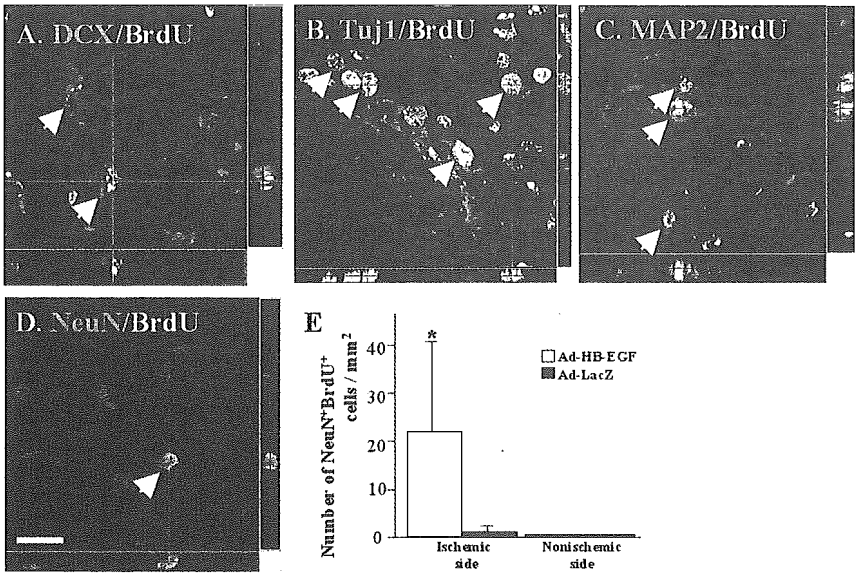

Figure 4. Differentiation of neuronal stem/progenitor cells. Some BrdU-positive cells in the ischemic striatum colocalized with DCX (A), Tuj1 (B), and MAP2 (C) at 28 days after MCAO. NeuN$^+$BrdU$^+$ cells were detected in Ad-HB-EGF–treated rats (D) but seldom detected in Ad-LacZ–treated rats (E). *$P<0.05$ vs Ad-LacZ–treated rats. Bar=20 μm in A through D.

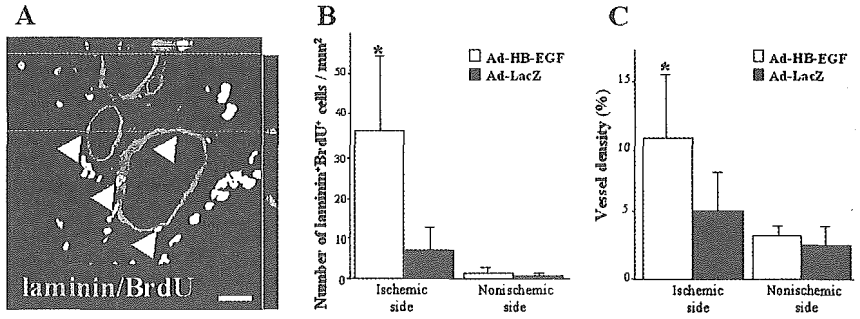

Figure 5. Angiogenesis in the striatum. Representative photograph shows that some BrdU-positive cells are laminin immunopositive in the ischemic striatum at 8 days after MCAO (A). Treatment with Ad-HB-EGF significantly increased laminin$^+$BrdU$^+$ cells (B) and vascular density (C) in the boundary regions of ischemia. *P<0.05 vs Ad-LacZ–treated rats. Bar=30 μm in A.

DCX (62±14%; Figure 4A), Tuj1 (37±13%; Figure 4B), and MAP2 (39±22%; Figure 4C) 28 days after ischemia. NeuN$^+$BrdU$^+$ cells were detected in the striatum 28 days after ischemia in the Ad-HB-EGF–treated rats (Figure 4D) but seldom detected in the Ad-LacZ–treated rats (22±18 versus 1±1 cell/mm^2; P<0.05; Figure 4E).

Treatment with Ad-HB-EGF significantly increased the number of laminin$^+$BrdU$^+$ cells (36±16 versus 6±6 cells/mm^2; P<0.05) and vascular density in the boundary regions of ischemia (10.7±4.6 versus 5.4±2.7%; P<0.05) compared with Ad-LacZ (Figure 5A through 5C).

Motor Function Recovery

MCAO caused marked impairment in the ability to remain on the rod 2 hours after ischemia. However, compared with the Ad-LacZ treatment group, the Ad-HB-EGF treatment group showed significant improvement in neurological outcome 14 days after MCAO (Figure 6).

Discussion

Recent studies have demonstrated that neurogenesis from endogenous precursors is induced in the striatum after focal cerebral ischemia.[18] Although it remains unknown whether new neurons are functional and integrated into the neural network, a novel therapeutic strategy for enhancing neurogenesis holds promise for functional recovery in stroke patients. The most promising approach for this purpose could be the administration of neurotrophic factors into the ischemic brain. In a normal rodent brain, the proliferation of neural stem cells and neuronal differentiation can be obtained after intraventricular administration of several growth factors such as EGF,[1] FGF-2,[2] BDNF,[3] and HB-EGF.[11] After Nakatomi's study showing regeneration of hippocampal neurons after ischemic injury by intraventricular administration of FGF-2 and EGF,[4] Teramoto et al demonstrated recently that intraventricular administration of EGF amplifies the proliferation of neural progenitors in SVZ and the replacement of striatal interneurons after MCAO.[5] However, dependence on chronic intraventricular catheterization into the lateral ventricle over a few days could cause infection, inflammation, and catheter loss that is inherent in chronic ventriculostomy. Gene therapy could overcome such disadvantage of protein delivery because single injection of viral vector into the lateral ventricle is expected to induce expression of desired molecule by infected cells for a long period. Several studies have also demonstrated that intracerebral or intraventricular injections of genes encoding neurotrophic factors could limit infarction size in the MCAO model.[19] However, to the best of our knowledge, only the *FGF-2* gene has been used in gene therapy for the purpose of increasing neurogenesis in the stroke model.[6] There is no evidence that *FGF-2* gene therapy in the MCAO model promotes neuronal differentiation from neural precursors in the striatum and cortex.

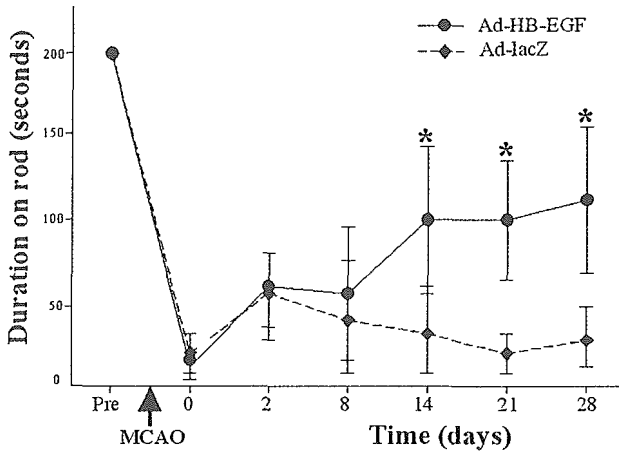

Figure 6. Motor function recovery. A repeated-measures ANOVA revealed that a significant interaction was found between treatment groups and time (days) for duration on rod (P<0.05). Mann–Whitney U test revealed that Ad-HB-EGF–treated rats showed significant improvement in neurological outcome evaluated by the rotarod test. *P<0.01 vs Ad-LacZ–treated rats at each time point. Each bar is the mean±SD.

In this study, we used adenovirus-mediated gene transfer of HB-EGF and demonstrated increased neurogenesis and angiogenesis in the striatum, and subsequent functional recovery in the rat after focal cerebral ischemia. The reasons we used *HB-EGF* gene are as follows. HB-EGF is a member of the EGF family, and EGF and HB-EGF have been shown to promote neurogenesis in vitro and in vivo.[1,11,20] However, HB-EGF binds to EGF-R/ErbB1 with higher affinity than that of EGF, and it also acts through EGF-insensitive receptor, including ErbB4[21] and *N*-arginine dibasic convertase (NRDc).[22] Because EGFR/ErbB1 and NRDc are expressed in the SVZ,[11] it is highly likely that HB-EGF stimulates neural progenitors at least as effectively as EGF. Although intraventricular administration of EGF might be better for increasing neurogenesis after ischemia than that of HB-EGF,[5,12] HB-EGF is also a mitogen for smooth muscle cells (SMCs) and a migration factor for SMCs and endothelial cells (ECs).[13] HB-EGF induces the secretion of vascular endothelial growth factor from SMCs, thus promoting proliferation of ECs.[13]

Therefore, the angiogenic property of HB-EGF is much stronger than that of EGF,[13] which could explain the increased angiogenesis by Ad-HB-EGF vector in this study.

In conclusion, the present study demonstrated that adenovirus-mediated gene transfer of HB-EGF promoted neurogenesis and angiogenesis in the striatum, and improved neurological functional recovery after focal ischemia. Postischemic gene therapy using the *HB-EGF* gene might be a potent therapeutic strategy to improve functional outcome in stroke patients.

Acknowledgments

The authors thank Dr S. Takashima (Osaka University Graduate School of Medicine, Japan) for kindly providing us with mouse HB-EGF cDNA, and Ms A. Kanzawa and S. Higa for secretarial assistance.

References

1. Craig CG, Tropepe V, Morshead CM, Reynolds BA, Weiss S, van der Kooy D. In vivo growth factor expansion of endogenous subependymal neural precursor cell populations in the adult mouse brain. *J Neurosci.* 1996;16:2649–2658.
2. Kuhn HG, Winkler J, Kempermann G, Thal LJ, Gage FH. Epidermal growth factor and fibroblast growth factor-2 have different effects on neural progenitors in the adult rat brain. *J Neurosci.* 1997;17:5820–5829.
3. Pencea V, Bingaman KD, Wiegand SJ, Luskin MB. Infusion of brain-derived neurotrophic factor into the lateral ventricle of the adult rat leads to new neurons in the parenchyma of the striatum, septum, thalamus, and hypothalamus. *J Neurosci.* 2001;21:6706–6717.
4. Nakatomi H, Kuriu T, Okabe S, Yamamoto S, Hatano O, Kawahara N, Tamura A, Kirino T, Nakafuku M. Regeneration of hippocampal pyramidal neurons after ischemic brain injury by recruitment of endogenous neural progenitors. *Cell.* 2002;110:429–441.
5. Teramoto T, Qiu J, Plumier JC, Moskowitz MA. EGF amplifies the replacement of parvalbumin-expressing striatal interneurons after ischemia. *J Clin Invest.* 2003;111:1125–1132.
6. Matsuoka N, Nozaki K, Takagi Y, Nishimura M, Hayashi J, Miyatake S, Hashimoto N. Adenovirus-mediated gene transfer of fibroblast growth factor-2 increases BrdU-positive cells after forebrain ischemia in gerbils. *Stroke.* 2003;34:1519–1525.
7. Goishi K, Higashiyama S, Klagsbrun M, Nakano N, Umata T, Ishikawa M, Mekada E, Taniguchi N. Phorbol ester induces the rapid processing of cell surface heparin-binding EGF-like growth factor: conversion from juxtacrine to paracrine growth factor activity. *Mol Biol Cell.* 1995;6:967–980.
8. Mishima K, Higashiyama S, Nagashima Y, Miyagi Y, Tamura A, Kawahara N, Taniguchi N, Asai A, Kuchino Y, Kirino T. Regional distribution of heparin-binding epidermal growth factor-like growth factor mrna and protein in adult rat forebrain. *Neurosci Lett.* 1996;213:153–156.
9. Nakagawa T, Sasahara M, Hayase Y, Haneda M, Yasuda H, Kikkawa R, Higashiyama S, Hazama F. Neuronal and glial expression of heparin-binding EGF-like growth factor in central nervous system of prenatal and early-postnatal rat. *Brain Res Dev Brain Res.* 1998;108:263–272.
10. Kawahara N, Mishima K, Higashiyama S, Taniguchi N, Tamura A, Kirino T. The gene for heparin-binding epidermal growth factor-like growth factor is stress-inducible: its role in cerebral ischemia. *J Cereb Blood Flow Metab.* 1999;19:307–320.
11. Jin K, Mao XO, Sun Y, Xie L, Jin L, Nishi E, Klagsbrun M, Greenberg DA. Heparin-binding epidermal growth factor-like growth factor: hypoxia-inducible expression in vitro and stimulation of neurogenesis in vitro and in vivo. *J Neurosci.* 2002;22:5365–5373.
12. Jin K, Sun Y, Xie L, Childs J, Mao XO, Greenberg DA. Post-ischemic administration of heparin-binding epidermal growth factor-like growth factor (HB-EGF) reduces infarct size and modifies neurogenesis after focal cerebral ischemia in the rat. *J Cereb Blood Flow Metab.* 2004;24:399–408.
13. Abramovitch R, Neeman M, Reich R, Stein I, Keshet E, Abraham J, Solomon A, Marikovsky M. Intercellular communication between vascular smooth muscle and endothelial cells mediated by heparin-binding epidermal growth factor-like growth factor and vascular endothelial growth factor. *FEBS Lett.* 1998;425:441–447.
14. Tanaka S, Kitagawa K, Sugiura S, Matsuoka-Omura E, Sasaki T, Yagita Y, Hori M. Infiltrating macrophages as in vivo targets for intravenous gene delivery in cerebral infarction. *Stroke.* 2004;35:1968–1973.
15. Swanson RA, Morton MT, Tsao-Wu G, Savalos RA, Davidson C, Sharp FR. A semiautomated method for measuring brain infarct volume. *J Cereb Blood Flow Metab.* 1990;10:290–293.
16. Sugiura S, Kitagawa K, Omura-Matsuoka E, Sasaki T, Tanaka S, Yagita Y, Matsushita K, Storm DR, Hori M. Cre-mediated gene transcription in the peri-infarct area after focal cerebral ischemia in mice. *J Neurosci Res.* 2004;75:401–407.
17. Sarnat HB. Histochemistry and immunocytochemistry of the developing ependyma and choroid plexus. *Microsc Res Tech.* 1998;41:14–28.
18. Arvidsson A, Collin T, Kirik D, Kokaia Z, Lindvall O. Neuronal replacement from endogenous precursors in the adult brain after stroke. *Nat Med.* 2002;8:963–970.
19. Toyoda K, Chu Y, Heistad DD. Gene therapy for cerebral vascular disease: update 2003. *Br J Pharmacol.* 2003;139:1–9.
20. Reynolds BA, Weiss S. Generation of neurons and astrocytes from isolated cells of the adult mammalian central nervous system. *Science.* 1992;255:1707–1710.
21. Elenius K, Paul S, Allison G, Sun J, Klagsbrun M. Activation of her4 by heparin-binding EGF-like growth factor stimulates chemotaxis but not proliferation. *EMBO J.* 1997;16:1268–1278.
22. Nishi E, Prat A, Hospital V, Elenius K, Klagsbrun M. *N*-arginine dibasic convertase is a specific receptor for heparin-binding EGF-like growth factor that mediates cell migration. *EMBO J.* 2001;20:3342–3350.

ELSEVIER

Atherosclerosis 179 (2005) 155–160

ATHEROSCLEROSIS

www.elsevier.com/locate/atherosclerosis

Associations of soluble intercellular adhesion molecule-1 with carotid atherosclerosis progression

Kimito Kondo[a,c], Kazuo Kitagawa[a,*], Yoji Nagai[a], Hiroshi Yamagami[a], Hiroyuki Hashimoto[b], Hidetaka Hougaku[a], Masatsugu Hori[a]

[a] *Department of Internal Medicine and Therapeutics, Osaka University Graduate School of Medicine (A8), 2-2 Yamadaoka, Suita, Osaka 5650871, Japan*

[b] *Department of Internal Medicine, Osaka National Hospital, Osaka, Japan*

[c] *Department of Cerebrovascular Medicine, Osaka Neurological Institute, Toyonaka, Japan*

Received 3 June 2004; received in revised form 10 September 2004; accepted 27 September 2004
Available online 14 November 2004

Abstract

Our previous study demonstrated that plasma concentration of high-sensitivity C-reactive protein (hs-CRP) is a marker of carotid atherosclerosis activity. In this study, we investigated whether plasma levels of soluble cell adhesion molecules have potential value to predict atherosclerosis progression. The study included 192 outpatients 40–82 years of age who were treated for traditional risk factor for cardiovascular disease. Patients underwent repeated ultrasonographic evaluation for 53 ± 11 months. Severity of atherosclerosis was evaluated by the maximal intimal-medial thickness (max-IMT), plaque number (PN) and plaque score (PS, the sum of all plaque thicknesses). Blood samples were collected for measurement of hs-CRP, soluble intercellular adhesion molecule (sICAM-1) and sP-selectin at the time of baseline examination. The development of atherosclerosis was estimated by the formula: Δvalue/year = (last value − baseline value)/number of follow-up years. Multivariate linear regression analysis revealed that sICAM-1 was associated with ΔIMT/year and ΔPS/year, which was not the case for sP-selectin. sICAM-1 was closely associated with ΔIMT/year especially in patients with apparent atheromatous plaque. Our results suggested that levels of sICAM-1 might have predictive value of progression of carotid atherosclerosis independently of traditional risk factors and hs-CRP.

Keywords: Intercellular adhesion molecule-1; C-reactive protein; Carotid atherosclerosis; P-selectin; Doppler ultrasound; Intimal-medial thickness; Plaque score

1. Introduction

Substantial advances in basic science have proven the fundamental role of inflammation and the underlying cellular and molecular mechanisms that contribute to atherogenesis [1]. In particular, the idea that atherosclerosis is a disorder characterized by low-grade vascular inflammation has received considerable attention. As a marker of such inflammation, high-sensitivity C-reactive protein (hs-CRP) has been a predictor of future cardiovascular events in several cohort studies [2]. Also, we have shown that the level of hs-CRP is predictive of carotid atherosclerosis progression, supporting the value of hs-CRP measurement in patients with cardiovascular risk factors [3]. Although hs-CRP is believed to be a general marker of inflammation, specific factors can contribute to the development of atherosclerosis. One of such factors is cell adhesion molecules [4]. Indeed, P-selectin is an adhesion receptor that mediates the initial rolling [5], where intercellular adhesion molecule-1 (ICAM-1) plays a critical role in the monocyte adherence to endothelial cells [6,7]. In line with such findings, deficiency of P-selectin or ICAM-1 is protective against atherosclerosis in apolipoprotein E-deficient mice [8,9]. Given that serum levels of soluble ICAM-1

* Corresponding author. Tel.: +81 6 6879 3634; fax: +81 6 6878 6574.
E-mail address: kitagawa@medone.med.osaka-u.ac.jp (K. Kitagawa).

0021-9150/$ – see front matter © 2004 Elsevier Ireland Ltd. All rights reserved.
doi:10.1016/j.atherosclerosis.2004.09.018

(sICAM-1) and soluble P-selectin (sP-selectin) move in parallel with their membrane level, sICAM-1 [10–12], and/or sP-selectin levels [13,14], in addition to hs-CRP levels [15,16], could be predictive of atherosclerotic diseases.

The development of B-mode ultrasound technique allows a noninvasive observation of atherosclerosis in vivo [17,18]. Although there are several cross-sectional studies relating sICAM-1 and sP-selectin levels to carotid atherosclerosis [19–23], longitudinal studies are limited. In the present longitudinal study, we investigated whether measurements of sICAM-1 and sP-selectin have potential value to predict atherosclerosis progression.

2. Methods

2.1. Patients

The subjects for this longitudinal study were enrolled from 216 patients of the Department of Internal Medicine and Therapeutics at Osaka University Hospital who had undergone carotid ultrasound examination between September 1996 and March 1998 because of the presence of risk factors for cardiovascular disease (CVD). The patients gave written informed consent to provide blood samples and undergo follow-up examinations for at least 3 years to evaluate the development of carotid atherosclerosis. The protocols were approved by the Osaka University Review Board. Patients were excluded from the study if they had experienced a clinical CVD event in the previous year or if another disease that could elevate the hs-CRP, sICAM-1 and sP-selectin concentration were present, i.e. malignancy, collagen disease, chronic renal failure, infection or hepatic disease. In the follow-up period, 8 patients suffered a new CVD event, and experienced no follow-up carotid survey. Another 6 patients suffered from malignant diseases, and 10 patients were lost to follow-up. A total of 24 patients experienced no follow-up carotid survey and were removed from the analyses. No patients were receiving antioxidant vitamin supplements, estrogen therapy, or steroid therapy.

2.2. Evaluation of carotid atherosclerosis

To evaluate the progression of carotid atherosclerosis, high-resolution B-mode ultrasonography with the use of 7.5 MHz duplex-type probe (EUB-525; Hitachi, Inc.) was performed repeatedly over a period of at least 3 years. Baseline and follow-up ultrasound images were recorded on Super VHS videotape, and the progression of atherosclerosis was evaluated, with clinical records blinded. We have measured the maximal intima-media thickness (max-IMT), plaque score (PS) and plaque number (PN), as indices of carotid atherosclerosis. All ultrasound images were obtained with the patient in supine position with the neck mildly extended and rotated to the contralateral side, and the measurement of IMT and PS was performed on the frozen frame, perpendicular to the vascular walls by scanning bilateral common and internal carotid arteries at the time of examination. IMT was measured as the greatest IMT in any parts of the far walls in carotid arteries including atheromatous plaques in both sides, and the unilateral max-IMT value, which was higher than the other side, was defined as max-IMT. PS and PN were calculated in accordance with our previous studies [3,18,21]. Based on our previous study, the upper limit of normal for IMT is 1.0 mm, and the lesions with a focal IMT $\geqq$ 1.1 mm were defined as atheromatous plaque. PS was calculated by summing all plaque thickness measurements in the both carotid arteries (Fig. 1). The progression of carotid atherosclerosis was estimated by the following formula for each parameter: Δvalue/year = (last value − baseline value)/number of follow-up years. When interobserver reproducibility was assessed for 20 patients, the interrater correlations of max-IMT, PS and PN were 0.90, 0.81 and 1.00, respectively. Early and mild stage of carotid atherosclerosis was defined as PS < 5 based on our grading system (moderate: 10 > PS $\geqq$ 5; severe: PS $\geqq$ 10, respectively).

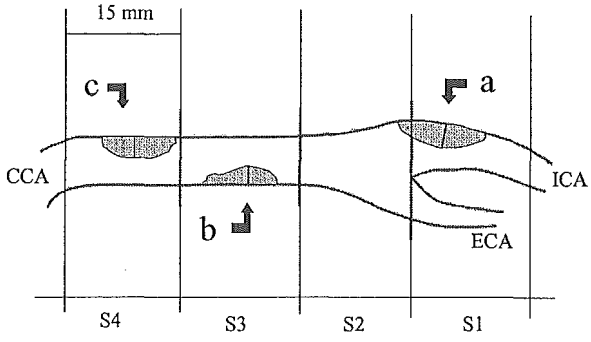

Fig. 1. Diagrams of carotid bifurcation and plaque score measurement obtained from B-mode ultrasonography. Plaque score was calculated by summing all plaque thickness in millimetres in each segment on both sides (a + b + c + contralateral plaques). Carotid artery was divided into four parts of 15 mm in length each from the flow divider (S1 to S4). CCA, common carotid artery; ICA, internal carotid artery; ECA, external carotid artery.

2.3. Measurement of circulating inflammatory markers

Blood samples were provided at the time of baseline carotid ultrasound examination and collected in tubes containing citric acid and EDTA, and were stored at −80 °C after centrifugation. The stored serum samples were assayed for sICAM-1, whereas the stored plasma samples were assayed for hs-CRP and sP-selectin. Commercially available monoclonal antibody-based ELISA kits (R&D Systems, Minneapolis, MN, U.S.A.) were used for the determination of sICAM-1 and sP-selectin levels. Levels of hs-CRP were measured by an automatic immunonephelometer with a sensitivity of 0.02 mg/dl (Behring NA latex CRP; Behring Institute). Measurements were made in pairs of samples from 20 patients about 1 year apart.

2.4. Definition of traditional risk factors for CVD

Hypertension was defined by systolic blood pressure ≧ 140 mmHg, diastolic blood pressure ≧ 90 mmHg or the current use of antihypertensive medications. Hypercholesterolemia was defined as a total cholesterol concentration ≧ 5.7 mmol/l, or the current use of cholesterol-lowering agents. Diabetes mellitus was defined as a glycosylated hemoglobin A1c concentration >5.8% or the current use of oral hypoglycemic agents. Cigarette pack-years were asked for each patient, to evaluate the cumulative exposure. Patients were categorized as having CVD if they had a prior history of ischemic heart disease, cerebrovascular disease, aortic aneurysm, or peripheral vascular disease.

2.5. Statistical analysis

All statistical analyses were performed with SPSS/Windows System, version 9.0J (SPSS Japan Inc.). Because distribution of hs-CRP levels was left-skewed, a natural log transformation was performed to achieve normality, which was used for subsequent analyses. In accordance with other studies [3,15,16], hs-CRP concentrations below the detection level were assigned a log-transformed value of −4.605 (hs-CRP value of 0.01 mg/dl). Relationships between inflammatory markers (hs-CRP, sICAM-1, sP-selectin) and carotid parameters (max-IMT, PS, PN) were examined by Pearson correlation analysis. Also, Mann–Whitney *U*-test was used to evaluate the difference between parameters by the presence or absence of traditional risk factors and statin use. Multiple linear regression analyses were used to assess the contributions of inflammatory markers to ΔIMT/year, ΔPS/year or ΔPN/year. Probability values were two-tailed and were considered significant when <0.05. For ease of interpretation, sICAM-1 concentrations were grouped in tertiles, and the differences in values were examined by one-way ANOVA followed by multiple comparisons test with Bonferroni's correction.

3. Results

Baseline characteristics of the study sample are shown in Table 1. Although prevalence of cardiovascular risk factors was generally high, they were relatively well controlled. The follow-up period was 53 ± 11 months, and 30% of our study patients had a CVD history. Levels of inflammatory markers had no significant difference between patients with and without a CVD history (sICAM-1: 208.4 versus 199.0 ng/ml; sP-selectin: 38.2 versus 38.3 ng/ml; hs-CRP: 0.113 versus 0.136 mg/dl, respectively; P = all n.s.). Among 20 patients who provided paired blood samples, the within-person correlation coefficients for s-ICAM-1, sP-selectin and hs-CRP were 0.858, 0.790 and 0.662, respectively. Baseline IMT and PS were not correlated with any inflammatory markers except that baseline PS was weakly correlated with sICAM-1 (Table 2). By contrast, both ΔIMT/year and ΔPS/year were significantly associated with sICAM-1 (r = 0.299 and 0.250, respectively), which was not the case for sP-selectin (Table 2). hs-CRP level was significantly associated only with ΔPS/year.

Table 1
Baseline characteristics

N	192
Age (years)	63.0 ± 8.6
Men (%)	51
Body mass index	23.3 ± 2.7
Hypertension/medical treatment (%)	73/62
Systolic/diastolic blood pressure (mmHg)	136 ± 18/81 ± 11
Hypercholesterolemia/medical treatment (%)	47/28
Total/HDL cholesterol (mmol/l)	5.37 ± 0.83/1.43 ± 0.42
Diabetes mellitus/medical treatment (%)	16/6
Fasting blood glucose (mmol/l)	5.82 ± 1.52
Hemoglobin A1c (%)	5.3 ± 0.8
Current smoking (%)	17
Brinkmann index	241.6 ± 467.3
History of CVD (%)	30
sICAM-1 (ng/ml)	202 ± 77
sP-selectin (ng/ml)	38 ± 22
hs-CRP (mg/dl, median)	0.13(0.07)
Max. IMT (mm)	1.74 ± 0.96
Plaque score (PS)	4.24 ± 4.86
Plaque number (PN)	2.40 ± 2.54
Follow-up period (months)	52.7 ± 11.2

Values are mean ± S.D. unless otherwise specified.

To further examine the associations between carotid atherosclerotic activity and serum inflammatory markers, multiple regression analyses were performed (Table 3). When controlling for age, sex, traditional risk factors and hs-CRP, sICAM-1 had significant associations with ΔIMT/year and ΔPS/year. Association of hs-CRP and ΔPS/year remained significant when controlling for age and sex (model 1), but such an association was of borderline significance when controlling for traditional risk factors (model 2). The associations between ΔIMT/year and sICAM-1 remained significant when noncurrent smokers (n = 159, β = 0.271, P = 0.001), patients without statin medication (n = 138, β = 0.353, P < 0.001) or patients without CVD history (n = 134, β = 0.321, P = 0.001) were analyzed separately on the basis of multivariate regression. For ease of interpretation, ΔIMT/year and ΔPS/year are shown in Fig. 2 in relation to sICAM-1 concentration tertiles. Both ΔIMT/year and ΔPS/year values in the highest tertile were significantly higher than values in the lowest tertile.

Because the development of new carotid plaques and progression of atheromatous plaques can show different patterns of associations with sICAM-1 and hs-CRP levels, we subsequently examined the associations in terms of plaque generation and progression. In 131 patients with early carotid atherosclerosis as defined by a PS < 5.0, ΔPN/year was analyzed to assess the development of new carotid plaques. Significant correlation was found between hs-CRP and ΔPN/year on the basis of simple regression, whereas sICAM-1 had no correlation with ΔPN/year (Table 4). On the other

Table 2
Associations of cardiovascular risk factors with baseline IMT, baseline PS, ΔIMT/year and ΔPS/year

	Baseline IMT	Baseline PS	ΔIMT/year	ΔPS/year
sICAM-1	0.088	0.146*	0.299**	0.250**
sP-selectin	0.090	0.140	0.085	0.113
hs-CRP	0.075	0.061	0.101	0.176*
Age	0.246**	0.352**	−0.087	0.055
Men/women	1.92 ± 1.15/1.57 ± 0.69*	5.01 ± 5.39/3.45 ± 4.12*	0.073 ± 0.196/0.044 ± 0.140	0.594 ± 0.892/0.375 ± 0.771
Hypertension, yes/no	1.79 ± 0.90/1.62 ± 1.12	4.65 ± 5.11/3.13 ± 3.93*	0.049 ± 0.149/0.083 ± 0.219	0.524 ± 0.862/0.381 ± 0.774
Hypercholesterolemia, yes/no	1.83 ± 1.04/1.67 ± 0.97	4.41 ± 4.59/3.89 ± 4.92	0.047 ± 0.160/0.065 ± 0.193	0.510 ± 0.882/0.413 ± 0.803
Diabetes mellitus, yes/no	2.03 ± 0.94/1.69 ± 1.01	4.41 ± 4.59/3.89 ± 4.92	0.078 ± 0.185/0.053 ± 0.177	0.510 ± 0.882/0.413 ± 0.803
Current smoking, yes/no	2.06 ± 1.43/1.69 ± 0.90*	5.80 ± 6.33/3.83 ± 4.38*	0.116 ± 0.237/0.046 ± 0.164*	0.834 ± 1.130/0.389 ± 0.760*
History of CVD, yes/no	1.95 ± 1.17/1.67 ± 0.93	4.92 ± 4.82/3.83 ± 4.73	0.072 ± 0.218/0.050 ± 0.161	0.503 ± 0.885/0.441 ± 0.824

Values represent correlation coefficients or mean ± S.D.
* $P < 0.05$.
** $P < 0.01$.

Table 3
Associations of ΔIMT/year and ΔPS/year with inflammatory markers and cardiovascular risk factors

	Simple regression		Model 1		Model 2		Model 3	
	r	*P*	*β*	*P*	*β*	*P*	*β*	*P*
ΔIMT/year								
sICAM-1	0.299	<0.001	0.301	<0.001	0.273	<0.001	0.265	0.001
hs-CRP	0.101	0.161	0.095	0.197	0.085	0.247	0.041	0.570
ΔPS/year								
sICAM-1	0.250	<0.001	0.230	0.002	0.198	0.010	0.178	0.022
hs-CRP	0.176	0.015	0.154	0.035	0.139	0.056	0.110	0.133

Model 1, age and sex are additionally controlled for; model 2, traditional cardiovascular risk factors are additionally controlled for; model 3, sICAM-1 and hs-CRP are additionally controlled for.

hand, ΔIMT/year was analyzed to assess the plaque progression in 105 patients with apparent atheromatous plaque as defined by a max-IMT ≧ 1.5. sICAM-1 had a significant correlation with ΔIMT/year both in simple regression ($r = 0.379$, $P < 0.001$) and multivariate regression ($\beta = 0.355$, $P < 0.001$), whereas its correlation with hs-CRP was not significant (Table 4).

4. Discussion

In the present study, we have demonstrated that sICAM-1 level is associated with the progression of carotid atherosclerosis as assessed by ΔIMT/year and ΔPS/year, whereas such association was not found for sP-selectin. Although both sICAM-1 and sP-selectin have been suggested to be a

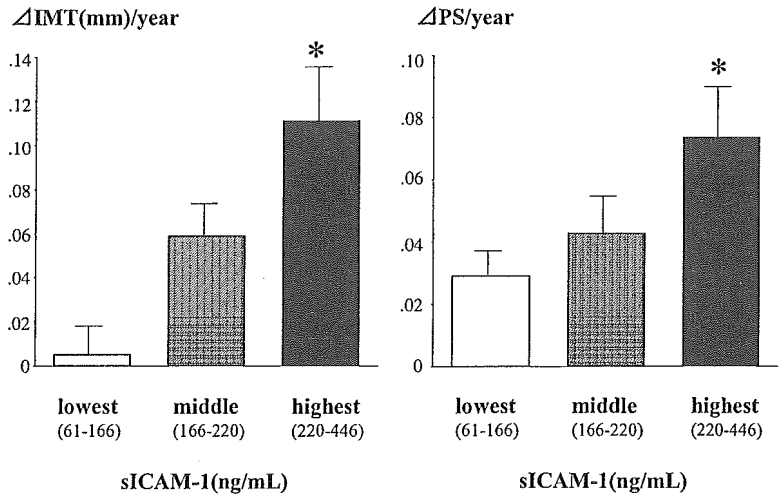

Fig. 2. Annual increase rate of carotid atherosclerosis according to tertiles of sICAM-1 levels. Bars represent means, and error bars represent S.E.M. ΔIMT/year and ΔPS/year in the highest tertile of sICAM-1 level were significantly higher than those in the lowest tertile (*$P < 0.05$).

Table 4
Associations between sICAM-1/hs-CRP Concentration and parameters associated with carotid atherosclerosis

	Simple regression		Multivariate regression	
	r	P	β	P
ΔPN/year per subgroup early carotid atherosclerosis (PS < 5), $n = 131$				
sICAM-1	0.107	0.222	0.010	0.911
hs-CRP	0.180	0.039	0.145	0.099
ΔIMT/year per subgroup apparent atheromatous plaque (IMT ≥ 1.5), $n = 105$				
sICAM-1	0.379	<0.001	0.355	<0.001
hs-CRP	0.159	0.105	0.180	0.085

Age, sex and traditional cardiovascular risk factors are controlled for multivariate regression model.

predictive marker for future cardiovascular events [10–14], it remains unclear whether the level of sICAM-1 or sP-selectin directly reflects the cell surface level of these molecules as a parameter of endothelial activation. In fact, little information is available regarding what regulates the production and catabolism of such molecules in vivo. However, increased endothelial ICAM-1 expression is reported in symptomatic carotid occlusion patients [24]. Also, we have suggested that the levels of sICAM-1 increased over time in parallel with the progression of atherosclerosis in apolipoprotein E-deficient mice, supporting the potential utility of sICAM-1 as an indicator of atherosclerosis progression [9]. Even when sICAM-1 level was not necessarily associated with endothelial ICAM-1 expression in patients who underwent carotid endarterectomy [25], endothelial ICAM-1 is shed into the plasma by proteolytic cleavage, making it likely that sICAM-1 levels reflect its membrane levels. Taken together, the association between sICAM-1 and ΔIMT/year or ΔPS/year as found in this study could be interpreted as an epiphenomenon occurring on the activated wall cell surface. By contrast, sP-selectin is derived from both platelet and endothelial cells. Because recent basic and clinical studies have shown the crucial role of platelet P-selectin, not sP-selectin, in atherosclerotic lesion development [26], the association of platelet P-selectin level with atherosclerosis progression needs to be clarified in future.

In the present study, we have demonstrated that sICAM-1 was associated with carotid atherosclerotic activity independently of traditional risk factors and hs-CRP. Although both sICAM-1 and hs-CRP correlated with atherosclerosis progression, their contribution may differ in the stages of atherosclerosis. As shown in our previous study [3], hs-CRP was associated with appearance of new carotid plaque in patients with early carotid atherosclerosis. However, it was not the case with sICAM-1 level. In contrast, sICAM-1 level correlated with progression of apparent atheromatous plaque, which was not the case with hs-CRP. Although hs-CRP is a useful marker for CVD events [2], it remains to be determined whether hs-CRP is the most reliable marker for low-grade inflammation involved in atherogenesis. Our results suggest each marker may have a respective significance and combined measurements of hs-CRP and sICAM-1 may have a potential utility to evaluate the activity of atherosclerosis progression. Among several cell adhesion molecules, we measured only sICAM-1 and sP-selectin, but other cell adhesion molecules such as vascular cell adhesion molecule (VCAM)-1 and E-selectin can also serve as markers for atherosclerosis. However, their implication for atherosclerosis and CVD events is controversial [10,20,27,28]. Also, factors that may influence the level of sICAM-1 may need to be considered when we interpret the association between sICAM-1 level and the progression of carotid atherosclerosis. For example, smoking can increase the level of sICAM-1 [29]. Additionally, medication usage could influence the level of sICAM-1. For instance, it has been demonstrated that statin therapy reduces the level of hs-CRP in a lipid-independent manner [30]. In the present study, the associations between sICAM-1 level and ΔIMT/year remained significant when subgroup analyses were performed for nonsmokers or for patients without statin usage, supporting the putative role of cell adhesion molecules in the evolution of atherosclerosis.

In conclusion, we have shown the association between sICAM-1 levels and the progression of carotid atherosclerosis independently of traditional risk factors and hs-CRP. Measurement of sICAM-1 may be of aid when predicting carotid atherosclerotic activity particularly in patients with apparent atheromatous plaque.

References

[1] Libby P, Ridker PM, Maseri A. Inflammation and atherosclerosis. Circulation 2002;105:1135–43.
[2] Pearson TA, Mensah GA, Alexander RW, et al. Markers of inflammation and cardiovascular disease application to clinical and public health practice. Circulation 2003;107:499–511.
[3] Hashimoto H, Kitagawa K, Hougaku H, et al. C-reactive protein is an independent predictor of the rate of increase in early carotid atherosclerosis. Circulation 2001;104:63–7.
[4] Frenette PS, Wagner DD. Molecular medicine: adhesion molecules. N Engl J Med 1996;334:1526–9.
[5] Frenette PS, Johnson RC, Hynes RO, Wagner DD. Platelets roll on stimulated endothelium in vivo: an interaction mediated by endothelial P-selectin. Proc Natl Acad Sci USA 1995;92:7450–4.
[6] Cybulsky MI, Gimbrone Jr MA. Endothelial expression of a mononuclear leukocyte adhesion molecule during atherogenesis. Science 1991;251:788–91.
[7] Adams DH, Shaw S. Leucocyte-endothelial interactions and regulation of leucocyte migration. Lancet 1994;343:831–6.
[8] Collins RG, Velji R, Guevara NV, Chan L, Beaudet AL. P-selectin or intercellular adhesion molecule-1 (ICAM)-1 deficiency substantially